

# Evaluation and LLM-Guided Learning of ICD Coding Rationales

Mingyang Li<sup>1</sup>, Viktor Schlegel<sup>2</sup>, Tingting Mu<sup>1</sup>, Wuraola Oyewusi<sup>1</sup>, Kai Kang<sup>3</sup>, Goran Nenadic<sup>1</sup>

<sup>1</sup>University of Manchester, <sup>2</sup>Imperial College London, <sup>3</sup>Shanxi Medical University  
 mingyang.li@manchester.ac.uk, v.schlegel@imperial.ac.uk, tingting.mu@manchester.ac.uk,  
 wuraola.oyewusi@postgrad.manchester.ac.uk, k.nikey0422@gmail.com, gnenadic@manchester.ac.uk

## Abstract

Automated clinical coding involves mapping unstructured text from Electronic Health Records (EHRs) to standardized code systems such as the International Classification of Diseases (ICD). While recent advances in deep learning have significantly improved the accuracy and efficiency of ICD coding, the lack of explainability in these models remains a major limitation, undermining trust and transparency. Current explorations about explainability largely rely on attention-based techniques and qualitative assessments by physicians, yet lack systematic evaluation using consistent criteria on high-quality rationale datasets, as well as dedicated approaches explicitly trained to generate rationales for further enhancing explanation. In this work, we conduct a comprehensive evaluation of the explainability of the rationales for ICD coding through two key lenses: faithfulness that evaluates how well explanations reflect the model’s actual reasoning and plausibility that measures how consistent the explanations are with human expert judgment. To facilitate the evaluation of plausibility, we construct a new rationale-annotated dataset, offering denser annotations with diverse granularity and aligns better with current clinical practice, and conduct evaluation across three types of rationales of ICD coding. Encouraged by the promising plausibility of LLM-generated rationales for ICD coding, we further propose new rationale learning methods to improve the quality of model-generated rationales, where rationales produced by prompting LLMs with/without annotation examples are used as distant supervision signals. We empirically find that LLM-generated rationales align most closely with those of human experts. Moreover, incorporating few-shot human-annotated examples not only further improves rationale generation but also enhances rationale-learning approaches.

## Introduction

Clinical coding is the process of translating free-text descriptions in patients’ Electronic Health Records (EHRs) into standardized codes, serving a critical role in billing, reimbursement, auditing, and decision support within healthcare systems (Blundell 2023). In this study, we focus on ICD coding—the document-level assignment of codes from the International Classification of Diseases (ICD) system (Tzitzivacos 2007), which provides hierarchical alphanumeric identifiers representing medical diagnoses and procedures.

Copyright © 2026, Association for the Advancement of Artificial Intelligence (www.aaai.org). All rights reserved.

Early ICD coding relied on manual efforts by trained professionals, which was costly, labor-intensive, and error-prone (Nguyen et al. 2018). To mitigate these challenges, rule-based systems were developed (Pereira et al. 2006; Crammer et al. 2007), followed by machine learning approaches such as Support Vector Machines (SVM) (Lita et al. 2008), which became the state of the art for a time. With the rise of deep learning, models like Gated Recurrent Units (GRUs) (Catling, Spithourakis, and Riedel 2018) and Convolutional Neural Networks (CNNs) (Karimi et al. 2017) substantially improved coding efficiency and accuracy. More recently, attention-based models (Liu et al. 2021; Van Aken et al. 2022; Yuan, Tan, and Huang 2022) and transformers (Michalopoulos et al. 2022; Yogarajan et al. 2022; Yang et al. 2022) have been adopted, consistently achieving new state-of-the-art results in clinical coding.

Although machine learning and deep learning methods have achieved notable success in ICD coding, their inherent lack of explainability poses a major challenge for understanding and interpreting model decisions. This limitation undermines trust and transparency, which are critical for enabling healthcare professionals and patients to confidently rely on AI-driven outcomes (Amann et al. 2020). To address this issue, researchers are increasingly developing methods that provide reliable explanations, often by extracting or generating short text snippets (*rationales*) e.g., based on attention mechanisms, and sometimes validating these explanations through physician assessment (Mullenbach et al. 2018).

Despite the growing exploration of rationale generation in ICD coding, there remain two main gaps: (a) a lack of systematic analysis of the explainability of these models using a high-quality rationale (evidence) dataset with a unified and aligned set of evaluation criteria which lead to (b) a lack of approaches focussed on rationale generation. In this study, we address this gap by introducing a new rationale dataset and conducting a comprehensive analysis of rationales generated to explain ICD coding, from two fundamental perspectives of faithfulness and plausibility. Furthermore, we propose effective rationale learning approaches and enhance rationale generation by leveraging this new dataset. Our key contributions are summarised below:

- We systematically evaluate the explainability quality rationales produced by state-of-the-art ICD coding models

equipped with label-wise attention mechanisms.

- We construct a new rationale dataset based on the up-to-date MIMIC-IV benchmark with ICD-10 codes for plausibility evaluation, providing richer rationales across multiple levels of granularity.
- We propose effective rationale learning approaches supervised by LLM-generated data, and demonstrate the utility of our rationale dataset to enhance LLM generation through few-shot prompting.

We show empirically that LLM-guided learning generates rationales more closely aligned with expert annotations, and the incorporation of human-annotated examples further improves rationale quality. We also observe a trade-off between the ICD coding classification performance and the rationale alignment with human annotations, informing future research that balancing both remains a challenging task.

## Related Work

**Rationale Snippets.** In one of the seminal studies on model explainability in clinical coding, Mullenbach et al. (2018) focus on extracting the most influential text snippets associated with predicted labels based on the importance values (attention weights) to  $n$ -grams in the input document assigned by the attention mechanism. They also extract rationales with the highest cosine similarity to code descriptions and take them as an additional explanation. Lovelace et al. (2020) follow the same idea, but apply attention mechanisms over multiple convolutional filters of different lengths, which allow them to consider variable spans of text. Yuan et al. (2021) also highlight the words based on the attention weights. Dong et al. (2021) build a Hierarchical Label-wise Attention Network (HLAN), which has label-wise word-level and sentence-level attention mechanisms, providing more comprehensive explanations for each label by highlighting key words and sentences in the discharge summaries. Wang et al. (2022) visualise the attention distribution to provide explanations. Similarly, Gao et al. (2024) design heatmap visualisation to help coders better understand the inference logic from EMR text.

**Evaluation Methods.** Mullenbach et al. (2018) evaluated the models’ effectiveness in identifying highly informative rationales by a physician’s assessment. Kim et al. (2022) assessed explainability using human-grounded evaluation, where annotators rated each explanation rationale for a predicted code as highly informative, informative, or irrelevant. Van Aken et al. (2022) evaluated explainability by faithfulness and conducted a manual analysis to judge whether highlighted tokens and prototypical patients aided decision-making. They only focused on three disease codes and compared the proposed model to post-hoc explanation methods, rather than other ICD coding baselines. For clinical coding the only existing rationale-annotated resource is (MDACE) Cheng et al. (2023). It evaluates the rationale extraction methods by exact and position independent token/span match.

**Data Limitation.** Being the only publicly available code rationale dataset, MDACE exhibits several limitations that

hinder its effectiveness for evaluating the explainability of ICD coding models. *Code Distribution Discrepancy:* MDACE is originally annotated with ICD-10 codes, subsequently mapped to the ICD-9. However, this mapping introduces a significant limitation: the resulting code distribution diverges markedly from that of standard MIMIC-III ICD-9 datasets used in ICD coding task. To quantify this discrepancy, we analyze code overlap under both the *Top-50* and *Full* code settings, observing average overlaps of only 37.00% and 14.59%, respectively. Notably, MDACE entirely omits 6 of the Top-50 codes and 725 out of 1,281 codes in the Full setting. This substantial inconsistency poses challenges in accurately evaluating the explainability of ICD coding models. Detailed statistics and analysis are provided in Appendix D. *Inaccuracies Arising from Mapping:* The mapping between ICD-9 and ICD-10 codes is not one-to-one, resulting in inaccuracies during conversion. In instances where multiple ICD-9 codes correspond to a single ICD-10 code, and none of the mapped codes appear in the original MIMIC-III ICD-9 dataset, the selection is guided by the textual similarity between ICD-9 and ICD-10 code descriptions. *Sparse Rationale Annotations:* Upon examining the quality of the annotations, we observe that most ICD codes are associated with very few supporting rationale annotations—often only a single instance. Such limited coverage is insufficient to represent the full spectrum of clinical rationale required for meaningful coding explanations. *Outdated Relevance of MIMIC-III:* Moreover, MIMIC-III has become increasingly outdated in the context of ICD coding. Contemporary research predominantly adopts the MIMIC-IV dataset, which employs the ICD-10 coding system, offering improved alignment with current clinical documentation standards and coding practices.

To improve the rationale evaluation, we develop a high-quality rationale annotation dataset with accurate code distributions, built on the up-to-date MIMIC-IV dataset with ICD-10 codes. We also propose effective LLM-guided learning approaches to improve rationale extraction, which are evaluated using this new rationale dataset.

## Preliminary on Explainable ICD Coding

ICD coding is treated as a multi-label classification task. It assigns ICD codes based on a patient’s clinical record, describing their diseases or procedures. We consider clinical documents, each of which is a discharge summary denoted as  $\mathbf{x}_i = \{\mathbf{t}_{i,1}, \mathbf{t}_{i,2}, \dots, \mathbf{t}_{i,N_i}\}$ , consisting of  $N_i$  tokens. The ICD coding model computes a label distribution over  $N_l$  labels for the input  $\mathbf{x}_i$ , i.e.,  $f(\mathbf{x}_i) = \mathbf{p}_i = [p_{i,1}, p_{i,2}, \dots, p_{i,N_l}]$ . The final codes are selected by thresholding the predicted probabilities with  $0 < \tau < 1$ , i.e.,

$$\hat{y}_{i,l} = \begin{cases} 1, & \text{if } p_{i,l} > \tau \\ 0, & \text{otherwise} \end{cases}, \text{ for } l = 1, 2, \dots, N_l.$$

To enable explainable ICD coding, the prediction models are expected to provide rationale explaining the decision making. The family of attention-driven ICD coding models achieves this by flagging key text rationales influential to the prediction using attention weights.

State-of-the-art attention-driven ICD coding models in-

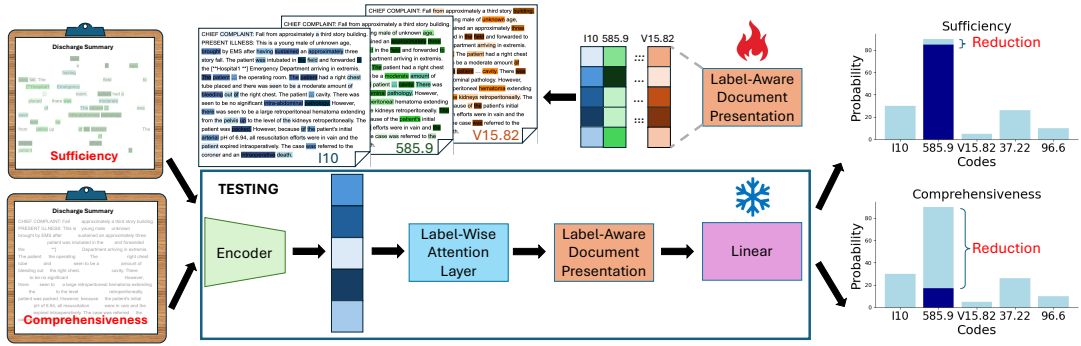


Figure 1: Faithfulness testing workflow. Sufficiency and comprehensiveness are evaluated by retaining or removing rationales from the original documents and using the modified texts as inputs to the trained ICD coding models.

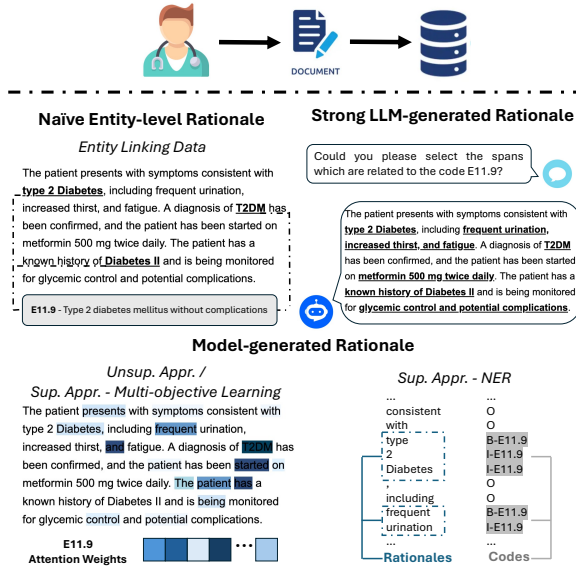


Figure 2: Examples of three types of rationales evaluated for plausibility. *Unsup. / Sup.* denote Unsupervised and Supervised, separately. *Appr.* indicates Approach.

clude CAML, LAAT and PLM-ICD. They compute an attention weight  $\tilde{a}_{i,j,l}$  for each token  $\mathbf{t}_{i,j}$  and for each label  $l$ . Specifically, CAML (Mullenbach et al. 2018) employs a single-filter CNN to encode the input text and computes the attention weight by  $\tilde{a}_{i,j,l} = \text{softmax}(\mathbf{u}_l^T \mathbf{t}_j)$ . LAAT (Vu, Nguyen, and Nguyen 2020) shares the same underlying framework as CAML, but leverages a BiLSTM to represent the input text  $\mathbf{x}_i$  and computes the attention weight by  $\tilde{a}_{i,j,l} = \text{softmax}(\mathbf{u}_l^T \tanh(\mathbf{W}_j \mathbf{t}_j))$ , introducing an additional weight matrix  $\mathbf{W}_j$ . PLM-ICD (Huang, Tsai, and Chen 2022) utilizes a transformer pre-trained on biomedical and clinical texts to encode the input text, and employs the same attention layer as LAAT. The attention weights are then used to compute a label-aware document representation by  $\tilde{\mathbf{h}}_{i,l} = \sum_{j=1}^{N_t} \tilde{a}_{i,j,l} \mathbf{t}_j$ . Together with the label representation vector  $\mathbf{z}_l$ ,  $\tilde{\mathbf{h}}_{i,l}$  is used to estimate the label probability by  $p_{i,l} = \sigma(\mathbf{z}_l^T \tilde{\mathbf{h}}_{i,l})$  through the sigmoid function

$\sigma$ . These models are trained by minimizing a binary cross-entropy loss:

$$\mathcal{L}_{\text{coding}} = -\frac{1}{N_D} \sum_{i=1}^{N_D} \sum_{l=1}^{N_l} [y_{i,l} \log \hat{y}_{i,l} + (1 - y_{i,l}) \log(1 - \hat{y}_{i,l})], \quad (1)$$

where  $N_D$  denotes the document number. Rationales are then extracted by selecting *top p%* tokens or *top N* tokens with the highest attention weights.

## An Empirical Analysis of ICD Rationales

### Evaluation Metrics

Explainability is typically evaluated from two complementary perspectives (Mendez Guzman, Schlegel, and Batista-Navarro 2024): a) Model-centric faithfulness, assessing how accurate the extracted rationales reflect the internal reasoning of the prediction models. b) Human-centric plausibility, measuring how convincing or intuitively acceptable the rationales appear to people.

**Faithfulness.** We denote the extracted rationale for explaining why input  $\mathbf{x}_i$  is predicted to label  $l$  by  $\hat{\mathbf{r}}_{i,l}$ . Its faithfulness can be assessed by two metrics, including **sufficiency** and **comprehensiveness** (DeYoung et al. 2019), quantifying the effect of perturbing or removing rationales, respectively. A rationale  $\hat{\mathbf{r}}_{i,l}$  is considered sufficient if it enables a prediction that closely approximates the one produced by using the full input  $\mathbf{x}_i$ . This motivates the sufficiency metric of  $\text{Suff} = P(f(\mathbf{x}_i)) - P(f(\hat{\mathbf{r}}_{i,l}))$ , where  $P(\cdot)$  denotes a used performance measure for ICD coding, e.g., classification accuracy, precision and recall, etc. Conversely, a highly comprehensive explanation should significantly impact the model prediction when the rationale  $\hat{\mathbf{r}}_{i,l}$  is removed. This motivates the comprehensiveness metric that measures the prediction change when the rationale  $\mathbf{r}_{i,l}$  is excluded from the input  $\mathbf{x}_i$ , computed as  $\text{Comp} = P(f(\mathbf{x}_i)) - P(f(\mathbf{x}_i \setminus \hat{\mathbf{r}}_{i,l}))$ . In general, lower sufficiency and higher comprehensiveness indicate better faithfulness.

**Plausibility.** A rationale is considered plausible when it highlights text rationales that are perceived by humans (e.g., domain experts) as relevant and appropriate to support model prediction. We assess plausibility by comparing the

Table 1: Statistics of RD-IV-10 and MDACE

Statistics	RD-IV-10	MDACE
Number of documents	150	363
Average length of documents	1690.63	1791.72
Average number of labels per document	14.82 / 16.15	11.53 / 17.10
Number of labels	2223 / 2422	4184 / 6208
Number of distinct labels	989 / 1044	1201 / 1381
Number of annotations	5391	5020
Average number of annotations per document	35.94	13.83
Average length of annotations	5.44	2.13

three types of rationales with human-annotated rationales, using the same matching metrics as in MDACE. To facilitate this, we construct an rationale dataset as below.

### Rationale Dataset Construction

We construct a new rationale dataset derived from MIMIC-IV and aligned with the ICD-10 coding system - **RD-IV-10**. This dataset includes detailed annotations capturing richer rationales supporting each code assignment, such as direct and indirect mentions, medications, and other pertinent clinical factors. Details of dataset construction, including Data Selection, Annotator, Annotation Guidelines, Annotation Platform, Inter-Annotator Agreement and Details of Data Processing are provided in Appendix C.

As shown in Table 1, the annotations in RD-IV-10 cover a significantly larger proportion of the original ICD labels compared to MDACE—an average of 14.52 out of 15.44 labels per document, versus 11.53 out of 17.10 in MDACE. We also report the specific labels for which no supporting rationale could be identified in Appendix C, offering further insight into the annotation quality of the MIMIC-IV ICD-10 dataset. Furthermore, our dataset provides substantially richer rationale: it includes an average of 35.16 rationale spans for 14.52 labels per document, whereas MDACE contains only 13.83 spans for 11.53 labels. Figure 3 further presents code-level statistics, showing that the number of annotations far exceeds the code frequency in the RD-IV-10 dataset. This confirms our earlier observation that MDACE typically offers only a single piece of supporting rationale per code. In addition, our dataset features more comprehensive annotation formats across multiple levels of granularity, including words, phrases, and both complete and partial sentences. The average length of each rationale span is also greater—5.00 tokens compared to 2.13 tokens in MDACE. A detailed case study comparing the annotation quality of the two datasets is presented in Appendix E. Additionally, some codes consistently have the highest number of annotations across both datasets, including I10, E785, E119, I2510, and others.

### Evaluation Method

We focus on examining the faithfulness of rationales extracted based on attention weights for CAML, LAAT and PLM-ICD. These are **model-generated rationales** produced with only supervision from ICD coding labels. The overall architecture for testing faithfulness is illustrated in

Figure 3: Statistics of top-10 codes in RD-IV-10 and MDACE

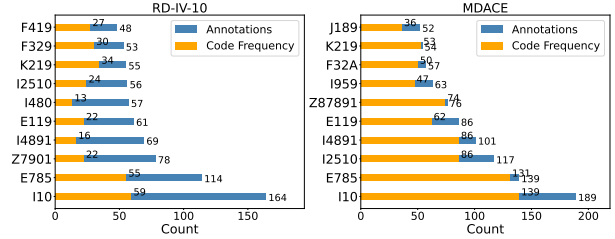


Figure 1. To analyze plausibility, we compare with two baseline ways of extracting rationales. One is a **naive extraction** by consulting an existing entity linking dataset, e.g., SNOMED CT Entity Linking Challenge dataset (Hardman et al. 2023). Such a dataset already links the ICD codes to relevant text mentions, e.g., entities like ‘*type 2 diabetes*’, ‘*T2DM*’, and ‘*Diabetes II*’ are linked to the ICD-10 code ‘*E11.9 – Type 2 diabetes mellitus without complications*’. When such entities appear in the input text  $x_i$ , they can directly serve as the rationale  $\hat{r}_{i,l}$  of the associated code  $l$ . The other is a **strong extraction**, which generates rationales by prompting a large language model (LLM). We prompt Gemini to extract rationale spans from patient notes that support specific ICD code assignments, and have observed that 2-Flash performs the best. Given that LLMs occasionally fail to produce spans that exactly match the original text, we design algorithms to align the generated spans back to the original document. Details of our prompt design and span alignment algorithm are provided in Appendix B. A thorough analysis of the comparison result is reported in the experiment section.

Encouraged by the promising plausibility of LLM-generated rationales, we propose to incorporate supervision from rationale labels generated by an LLM, e.g., the best-performing Gemini 2-Flash, and explain the methodology in the next section. Figure 2 presents an example of each type of rationale.

### LLM-Guided Rationale Learning

LLMs have demonstrated strong performance across a variety of tasks in the clinical domain. Also, we have observed from the previous rationale analysis that the LLM-generated rationales align quite well with human-annotated rationales. This motivates us to take advantage of LLMs, i.e., being able to quickly identify rationale with reasonable quality, and design LLM-guided rationale learning approaches. We propose to use rationales produced by prompting LLMs as distant supervision signal, aiming at maximizing simultaneously classification accuracy for ICD coding and plausibility of the model-generated rationales.

**Multi-objective Learning** One way to embed rational learning into ICD coding is to incorporate another learning objective alongside the primary classification objective of the ICD coding model, minimizing the discrepancy between the model-generated rationales (controlled by attention weights) and the provided rationale labels by LLMs.

We define the rationale labels associated with a code label  $l$  as  $\mathbf{r}_{il}$ . To represent these rationales, we construct a binary mask matrix  $\mathbf{M}_{i,l}$ , where a value of 1 indicates that the corresponding token is part of the rationale, and 0 otherwise. We design the following rationale generation loss by applying binary cross-entropy to the attention weights and rationale masks:

$$\mathcal{L}_{\text{rationale}} = -\frac{1}{N_D} \sum_{i=1}^{N_D} \sum_{l=1}^{N_l} \sum_{j=1}^{N_t} [M_{i,l,j} \log \tilde{a}_{i,j,l} + (1 - M_{i,l,j}) \log(1 - \tilde{a}_{i,j,l})] \quad (2)$$

The final ICD coding model is trained by minimizing the combined loss of  $\mathcal{L}_{\text{coding}} + \mathcal{L}_{\text{rationale}}$ .

**Learning by NER Formulation** An alternative approach to enable both rationale and ICD code learning is to leverage the rationale labels provided by LLMs to train a named-entity recognition (NER) model (Yang et al. 2020). Specifically, each rationale is treated as an entity with its corresponding ICD code assigned as its class label, while text that is not identified as a rationale is assigned a null class. The success of entity recognition contributes to both ICD code classification and rationale extraction. As a result, the ICD coding and rationale learning tasks are neatly converted to one single NER task, solved by following the standard NER training.

**Enhanced Supervision by Few-shot Prompting** Manual rationale annotation is time-consuming and costly, limiting scalability to large datasets. Although LLMs provide a promising alternative for automatic annotation, they are susceptible to hallucinations and inaccuracies (Li et al. 2023; Ji et al. 2023), particularly in expert domains such as healthcare (Nagar et al. 2024). Prior studies have shown that few-shot prompting, where models are provided with few examples, can substantially improve generation quality (Sivarajkumar et al. 2024). Motivated by this, we further incorporate a small amount of example annotations provided by our constructed rationale dataset into the prompts of Gemini 2-Flash. Details of the prompt design are provided in Appendix B. The rationales obtained from the enhanced prompts are then used to supervise the rationale learning.

## Experiments and Result Analysis

We conduct evaluation using both the MIMIC-III dataset with ICD-9 codes and the more recent MIMIC-IV benchmark with ICD-10 codes. To assess the ICD coding performance, we use F1, AUC, and Precision@N, following the standard practice. To conduct experiments on plausibility, we use the SNOMED CT Entity Linking Challenge dataset (Hardman et al. 2023) to implement the naive rationale extraction, i.e., entity-level rationales. We compare both cloud-based and locally deployed LLMs, including Gemini 2-Flash, Gemini 1.5-Pro and LLaMA-3.3, to implement the strong rationale extraction, i.e., LLM-generated rationales<sup>1</sup>.

<sup>1</sup>To support further research, the complete Gemini-generated rationale dataset covering 120K documents in MIMIC-IV ICD-10 will be made publicly available upon publication of this paper.

To ensure a fair comparison between the three models of CAML, LAAT and PLM-ICD, we follow the experimental setup of a reproducibility framework Edin et al. (2023). We implement NER models under the default hyperparameter settings in Yang et al. (2020). More details on datasets and implementations are provided in Appendices A and B.

## Comparison of ICD Rationales

**Faithfulness of CAML, LAAT and PLM-ICD: How Explainable Are Rationales to Machines?** Figure 4 compares the faithfulness of the three ICD coding models with *Top N tokens* rationale selection strategy. Results are reported in terms of precision@5 for the Top-50 datasets and precision@8 for the Full datasets. More results across more metrics with both *Top N tokens* and *Top p% tokens* are reported in Appendix F.

For sufficiency, **PLM-ICD performs comparably to LAAT, and both models outperform CAML** on the MIMIC-IV ICD-10 Full dataset as well as the two MIMIC-III ICD-9 datasets. PLM-ICD achieves the highest sufficiency using only 200 tokens, with a 10% and 25% performance drop on the Top-50 and Full datasets, respectively. As these tokens represent just 11–16% of the input text, this highlights substantial noise in the data and PLM-ICD’s ability to focus on the most influential rationales. For comprehensiveness, **removing rationales causes the greatest performance drop in LAAT**, particularly on the MIMIC-IV ICD-10 Full and two MIMIC-III ICD-9 datasets. In contrast, PLM-ICD shows smaller declines, even less than CAML on the ICD-9 datasets, suggesting that its pre-training enhances robustness by effectively extracting relevant information from residual inputs.

## Plausibility of Naive, Strong and Model-generated Rationales: How Explainable Are Rationales to Experts?

Table 2 summarises the plausibility results across different types of rationales. The results show that model-generated rationale yield the lowest metric scores, entity-level rationales rank second, while LLM-generated rationales perform the best, with Gemini 2-Flash achieving the highest scores. An additional case study comparing these rationales with human annotations is provided in Appendix H.

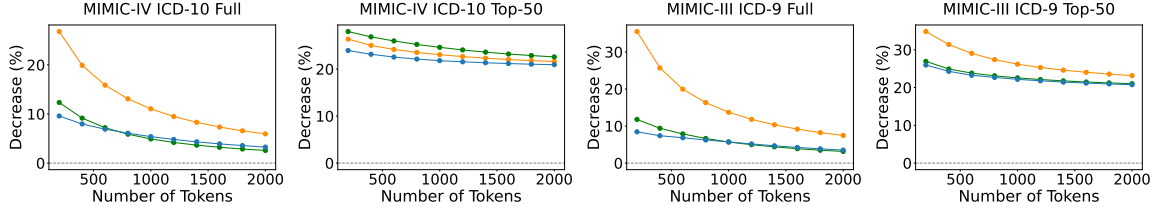
## Naive Rationales: Are Linked Entities Sufficient to Serve as Rationales?

The performance of directly linked entities ranks in the middle among the three types of rationales. However, its actual matching quality is underestimated, as the entity linking and MIMIC-IV ICD-10 dataset use different coding schemes despite referring to the same clinical mentions. For instance, in sample HADM ID: 24813967, all occurrences of ‘fall’ are assigned ‘R29.6 – Repeated falls’, whereas MIMIC-IV ICD-10 labels the case with ‘W01.0XXA – Fall on same level from slipping, tripping and stumbling without subsequent striking against object, initial encounter’. **In conclusion, directly linked entities can serve as rationales to a certain extent.**

**Strong Rationales: Can LLMs Generate High-Quality Rationales?** The Gemini 2-Flash model achieves the highest performance among all comparisons. However,



Sufficiency of Models on Four MIMIC Datasets (Precision@5/8)



Comprehensiveness of Models on Four MIMIC Datasets (Precision@5/8)

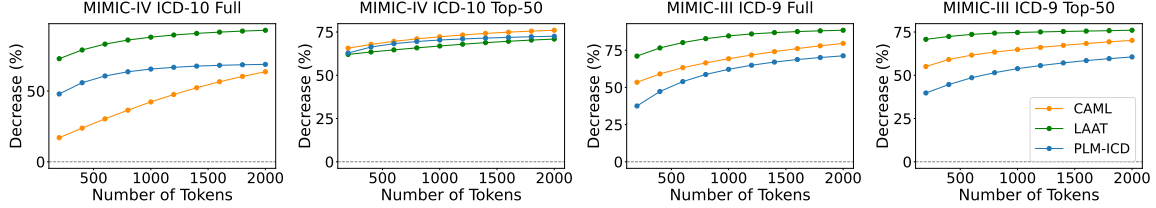


Figure 4: Faithfulness results of ICD coding models on four MIMIC datasets (precision@5/8).

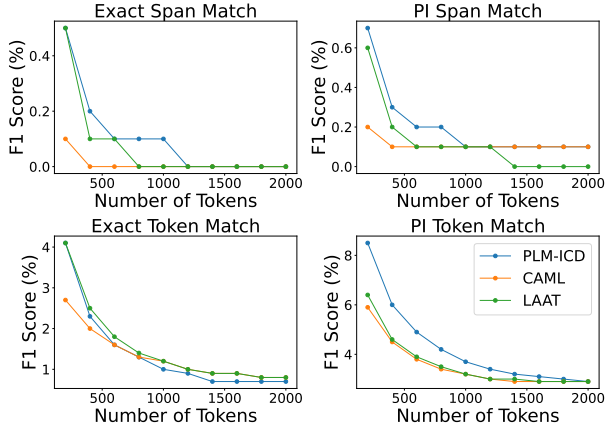


Figure 5: Plausibility results of ICD coding models across all thresholds settings.

both more cost-effective local LLaMA-3.3 models deliver competitive results, with only a minor drop observed in the quantized variant AWQ. Importantly, the AWQ requires significantly fewer computational resources—approximately 40 GB of memory, compared to the Instruct model, which necessitates  $4 \times A100$  80 GB GPUs in this case.

**Model-generated Rationales: Do Tokens with Higher Attention Weights Make Sense?** Figure 5 reports the matching results of *Top N tokens* across all thresholds. Overall, the performances of the three models are comparable. Specifically, PLM-ICD demonstrates better plausibility than LAAT, which in turn outperforms CAML. Span-level matches remain close to zero across all thresholds. Models achieve higher scores at lower thresholds, because shorter spans are selected, which better align with human annotations. For token-level matches, the absolute number of true positives increases at higher thresholds due to the inclusion of more tokens. However, the F1 scores decline because the

Table 4: ICD coding performance of LLM-guided supervised approaches. The experiments are conducted on the Top-50 code settings. All results are reported as percentages.

Model	F1-Mac	F1-Mic	P-Mac	P-Mic	R-Mac	R-Mic
PLM-ICD	68.18	73.40	68.71	73.48	69.38	73.33
Multi-objective	67.93	73.26	67.60	72.66	69.53	73.87
PLM-ICD	61.09	68.18	60.06	67.62	63.90	68.76
NER	53.46	67.75	49.21	60.93	61.79	76.30

total number of predicted tokens increases more substantially than the number of true positives. **In conclusion, the rationales generated by ICD coding models do not align with human explanations.** More results on these are provided in Appendix F.

## Results for LLM-Guided Rationale Learning

**Standard Prompting: Does It Improve ICD Coding Performance and Rationale Plausibility?** Tables 2 and 3 compare the plausibility and ICD coding performance for the PLM-ICD model before and after introducing LLM-guided rationale learning, respectively. For the multi-objective learning, it can be seen from Table 3 that the LLM guidance enhances the plausibility of the generated rationales, leading to stronger alignment with human-annotated rationales. However, there is a slight drop of the ICD coding performance as seen in Table 4, caused by the incorporation of the additional learning objective. For the NER-based approach, Table 3 demonstrates that its recognized spans achieve the highest span-level plausibility, even surpassing that of its ‘teacher model’ - Gemini 2-Flash. This finding suggests that Gemini-generated rationale labels are sufficient for training a rationale recognition model, and that such a model can be freely deployed. However, the NER model exhibits substantially lower overall coding performance than PLM-ICD as shown in Table 4. **Overall, we observe this interesting trade-off between the ICD coding**

Table 2: Document-level and code-level plausibility results (F1) of **naive entity-level rationales**, **strong LLM-generated rationales**, **model-generated rationales (no supervision)**. 200 denotes selected tokens, “w/o” and “w/” indicate the absence or inclusion of few-shot examples in prompts. All results are reported as percentages.

Model / Code	Settings	Exact SM	PI SM	Exact TM	PI TM
<b>Document-level Evaluation</b>					
Entity-Linking	–	10.3	9.2	6.3	6.1
Gemini 2-Flash	–	<b>21.6</b>	<b>24.1</b>	<b>30.1</b>	<b>37.3</b>
Gemini 1.5-Pro	–	13.5	14.6	20.6	26.0
LLaMA-3.3 Ins	–	18.6	21.5	27.8	35.0
LLaMA-3.3 AWQ	–	17.5	20.1	27.2	34.1
CAML	200	0.1	0.2	3.1	6.5
LAAT	200	0.7	0.8	5.0	7.2
PLM-ICD	200	0.5	0.7	4.3	8.8
<b>Code-level Evaluation (Gemini 2-Flash)</b>					
I10	w/o	50.3	63.1	27.0	32.2
	w/	<b>60.5</b>	<b>78.2</b>	<b>53.8</b>	<b>66.4</b>
E785	w/o	62.5	76.6	50.2	59.7
	w/	<b>73.2</b>	<b>89.5</b>	<b>66.7</b>	<b>78.2</b>
Z7901	w/o	9.0	9.7	35.8	43.3
	w/	<b>13.0</b>	<b>16.8</b>	<b>45.8</b>	<b>54.8</b>
I4891	w/o	11.8	16.7	28.0	34.8
	w/	<b>24.7</b>	<b>36.9</b>	<b>47.9</b>	<b>56.2</b>
E119	w/o	40.8	48.8	36.2	37.4
	w/	<b>44.2</b>	<b>52.9</b>	<b>43.6</b>	<b>44.8</b>

**performance and rationale plausibility, which is natural due to the increased difficulty of the joint learning tasks.**

**Few-shot Prompting: Does It Improve Plausibility of LLM-Generated Rationales?** In the code-level evaluation, we conduct experiments on the five most frequent codes in the dataset: I10, E785, Z7901, I4891, and E119. We analyze rationales generated by Gemini 2-Flash with and without few-shot examples in the prompts to also examine whether incorporating example annotations can further enhance Gemini’s performance. In the few-shot experiments, five human-annotated samples per code are added to the prompts, and Gemini regenerates rationales for the remaining samples, which are then re-evaluated using the same plausibility metrics. **Incorporating examples yields substantial improvements in F1 scores** across all five codes shown in Table 3, with average gains of 39.90%, 48.67%, 50.31%, and 49.01% in Exact Span Match, PI Span Match, Exact Token Match, and PI Token Match, respectively. These results demonstrate the effectiveness of our rationale dataset in enhancing rationale generation. More results for this experiment are provided in Appendix G.

**Few-shot Prompting: Does It Improve LLM-Guided Rationale Learning?** Building on our previous experiments and analyses, which demonstrated that incorporating few-shot examples in prompts enhances rationale generation, this experiment investigates whether these enhanced rationales can improve the training of NER models for rationale recognition. Specifically, we train separate NER models using Gemini-generated rationales, both with and without few-shot examples in the prompts, for each of the five most frequent codes. The rationale plausibility results are reported in the bottom half of Table 3.

Table 3: Document-level and code-level plausibility results (F1) of LLM-guided supervised approaches. The experiments for multi-objective learning and NER are conducted on different datasets using the Top-50 code settings. 50 denotes selected tokens, “w/o” and “w/” indicate the absence or inclusion of few-shot examples in prompts. **when constructing the training datasets**. All results are reported as percentages.

Model	Settings	Exact SM	PI SM	Exact TM	PI TM
<b>Document-level Evaluation</b>					
PLM-ICD	50	2.7	3.0	9.5	12.2
Multi-objective	50	<b>3.9</b>	<b>4.1</b>	<b>10.6</b>	<b>13.2</b>
PLM-ICD	50	4.1	4.3	8.1	12.0
Gemini 2-Flash	–	18.2	23.0	<b>29.4</b>	<b>31.4</b>
NER	–	<b>26.5</b>	<b>30.6</b>	21.8	27.0
<b>Code-level Evaluation (NER)</b>					
I10	w/o	55.4	76.9	55.8	75.3
	w/	<b>62.5</b>	<b>85.2</b>	<b>64.9</b>	<b>86.2</b>
E785	w/o	67.9	85.5	61.6	75.2
	w/	<b>70.3</b>	<b>87.0</b>	<b>63.0</b>	<b>76.3</b>
Z7901	w/o	10.3	<b>13.8</b>	<b>25.5</b>	38.6
	w/	<b>10.8</b>	12.0	22.5	<b>40.7</b>
I4891	w/o	22.2	37.7	38.5	48.8
	w/	<b>26.1</b>	<b>43.3</b>	<b>40.7</b>	<b>54.5</b>
E119	w/o	<b>49.4</b>	<b>62.0</b>	<b>53.2</b>	<b>62.4</b>
	w/	45.8	58.5	49.7	60.2

Table 3 shows that the **NER formulation is effective for single code rationale recognition**. It significantly outperforms the teacher models (w/o results in Table 2) across all codes and metrics, achieving average improvements of 28.49%, 45.71%, 37.01%, and 51.21% on the four metrics, respectively. Among all codes, E785 and I10 achieve higher performance, which is attributed to the higher frequency of occurrence of codes and their associated rationales within the documents, thereby benefiting model training. Furthermore, **the model trained on data generated with few-shot examples in the prompts consistently outperforms the one trained without such examples in most cases**, with average improvements of 6.30%, 1.74%, 1.19%, 5.91%. This further demonstrates that the RD-IV-10 effectively guides Gemini’s generation process, enhancing the plausibility of the generated rationales.

## Conclusion and Future Work

In this study, we evaluate the explainability of ICD coding models from their faithfulness and plausibility. We introduce a high-quality rationale dataset and use it to evaluate the plausibility of three types of rationales. We also propose LLM-guided rationale-learning approaches. Our findings show that LLM-generated rationales achieve the highest plausibility, and that incorporating human-annotated examples into prompts not only improves rationale generation but also enhances rationale-learning processes.

Our work has several limitations. First, the evaluation of naive entity-level rationales could be improved by aligning coding schemes more precisely. Second, our NER models are trained on relatively small datasets of 5,000 randomly selected samples due to time constraints; future work could involve experiments on the Full datasets. Finally, our results

reveal a trade-off between the decrease in ICD coding performance and the improvement in rationale generation—an intriguing phenomenon that warrants further investigation.

## References

- Amann, J.; Blasimme, A.; Vayena, E.; Frey, D.; Madai, V. I.; and Consortium, P. 2020. Explainability for artificial intelligence in healthcare: a multidisciplinary perspective. *BMC medical informatics and decision making*, 20: 1–9.
- Blundell, J. 2023. Health information and the importance of clinical coding. *Anaesthesia & Intensive Care Medicine*, 24(2): 96–98.
- Catling, F.; Spithourakis, G. P.; and Riedel, S. 2018. Towards automated clinical coding. *International journal of medical informatics*, 120: 50–61.
- Cheng, H.; Jafari, R.; Russell, A.; Klopfer, R.; Lu, E.; Striner, B.; and Gormley, M. R. 2023. MDACE: MIMIC Documents Annotated with Code Evidence. *arXiv preprint arXiv:2307.03859*.
- Crammer, K.; Dredze, M.; Ganchev, K.; Talukdar, P.; and Carroll, S. 2007. Automatic code assignment to medical text. In *Biological, translational, and clinical language processing*, 129–136.
- DeYoung, J.; Jain, S.; Rajani, N. F.; Lehman, E.; Xiong, C.; Socher, R.; and Wallace, B. C. 2019. ERASER: A benchmark to evaluate rationalized NLP models. *arXiv preprint arXiv:1911.03429*.
- Dong, H.; Suárez-Paniagua, V.; Whiteley, W.; and Wu, H. 2021. Explainable automated coding of clinical notes using hierarchical label-wise attention networks and label embedding initialisation. *Journal of biomedical informatics*, 116: 103728.
- Edin, J.; Junge, A.; Havtorn, J. D.; Borgholt, L.; Maistro, M.; Ruotsalo, T.; and Maaløe, L. 2023. Automated medical coding on MIMIC-III and MIMIC-IV: a critical review and replicability study. In *Proceedings of the 46th international ACM SIGIR conference on research and development in information retrieval*, 2572–2582.
- Gao, Y.; Chen, Y.; Wang, M.; Wu, J.; Kim, Y.; Zhou, K.; Li, M.; Liu, X.; Fu, X.; Wu, J.; et al. 2024. Optimising the paradigms of human AI collaborative clinical coding. *npj Digital Medicine*, 7(1): 368.
- Hardman, W.; Banks, M.; Davidson, R.; Truran, D.; Ayuningtyas, N. W.; Ngo, H.; Johnson, A.; and Pollard, T. 2023. SNOMED CT Entity Linking Challenge. *PhysioNet. Version*, 1(0).
- Huang, C.-W.; Tsai, S.-C.; and Chen, Y.-N. 2022. PLM-ICD: Automatic ICD coding with pretrained language models. *arXiv preprint arXiv:2207.05289*.
- Ji, Z.; Lee, N.; Frieske, R.; Yu, T.; Su, D.; Xu, Y.; Ishii, E.; Bang, Y. J.; Madotto, A.; and Fung, P. 2023. Survey of hallucination in natural language generation. *ACM computing surveys*, 55(12): 1–38.
- Johnson, A.; Bulgarelli, L.; Pollard, T.; Horng, S.; Celi, L. A.; and Mark, R. 2020. MIMIC-IV. *PhysioNet*. Available online at: <https://physionet.org/content/mimiciv/1.0/> (accessed August 23, 2021), 49–55.
- Karimi, S.; Dai, X.; Hassanzadeh, H.; and Nguyen, A. 2017. Automatic diagnosis coding of radiology reports: a comparison of deep learning and conventional classification methods. In *BioNLP 2017*, 328–332.
- Kim, B.-H.; Deng, Z.; Yu, P. S.; and Ganapathi, V. 2022. Can current explainability help provide references in clinical notes to support humans annotate medical codes? *arXiv preprint arXiv:2210.15882*.
- Li, J.; Cheng, X.; Zhao, W. X.; Nie, J.-Y.; and Wen, J.-R. 2023. Halueval: A large-scale hallucination evaluation benchmark for large language models. *arXiv preprint arXiv:2305.11747*.
- Lita, L. V.; Yu, S.; Niculescu, S.; and Bi, J. 2008. Large scale diagnostic code classification for medical patient records. In *Proceedings of the Third International Joint Conference on Natural Language Processing: Volume-II*.
- Liu, Y.; Cheng, H.; Klopfer, R.; Gormley, M. R.; and Schaaf, T. 2021. Effective convolutional attention network for multi-label clinical document classification. In *Proceedings of the 2021 Conference on Empirical Methods in Natural Language Processing*, 5941–5953.
- Lovelace, J.; Hurley, N. C.; Haimovich, A. D.; and Mortazavi, B. J. 2020. Dynamically extracting outcome-specific problem lists from clinical notes with guided multi-headed attention. In *Machine Learning for Healthcare Conference*, 245–270. PMLR.
- Mendez Guzman, E.; Schlegel, V.; and Batista-Navarro, R. 2024. From outputs to insights: a survey of rationalization approaches for explainable text classification. *Frontiers in Artificial Intelligence*, 7: 1363531.
- Michalopoulos, G.; Malyska, M.; Sahar, N.; Wong, A.; and Chen, H. 2022. ICDBigBird: a contextual embedding model for ICD code classification. *arXiv preprint arXiv:2204.10408*.
- Mullenbach, J.; Wiegrefe, S.; Duke, J.; Sun, J.; and Eisenstein, J. 2018. Explainable prediction of medical codes from clinical text. *arXiv preprint arXiv:1802.05695*.
- Nagar, A.; Liu, Y.; Liu, A. T.; Schlegel, V.; Dwivedi, V. P.; Kaliya-Perumal, A.-K.; Kalanchiam, G. P.; Tang, Y.; and Tan, R. T. 2024. umedsum: A unified framework for advancing medical abstractive summarization. *arXiv preprint arXiv:2408.12095*.
- Nguyen, A. N.; Truran, D.; Kemp, M.; Koopman, B.; Conlan, D.; O'Dwyer, J.; Zhang, M.; Karimi, S.; Hassanzadeh, H.; Lawley, M. J.; et al. 2018. Computer-assisted diagnostic coding: effectiveness of an NLP-based approach using SNOMED CT to ICD-10 mappings. In *AMIA Annual Symposium Proceedings*, volume 2018, 807. American Medical Informatics Association.
- Pereira, S.; Névél, A.; Massari, P.; Joubert, M.; and Darmoni, S. 2006. Construction of a semi-automated ICD-10 coding help system to optimize medical and economic coding. In *MIE*, 845–850.
- Sivarajkumar, S.; Kelley, M.; Samolyk-Mazzanti, A.; Visweswaran, S.; and Wang, Y. 2024. An empirical evaluation of prompting strategies for large language models in



zero-shot clinical natural language processing: algorithm development and validation study. *JMIR Medical Informatics*, 12: e55318.

SNOMED-CT. 2024. SNOMED CT U.S. Edition Release, September 1, 2024. [https://www.nlm.nih.gov/healthit/snomedct/us\\_edition.html](https://www.nlm.nih.gov/healthit/snomedct/us_edition.html). File: der2\_iisssccRefset\_ExtendedMapFull\_US1000124\_20240901.txt.

Tzitzivacos, D. 2007. International classification of diseases 10th edition (icd-10). *CME: Your SA Journal of CPD*, 25(1): 8–10.

Van Aken, B.; Papaioannou, J.-M.; Naik, M. G.; Eleftheriadis, G.; Nejdil, W.; Gers, F. A.; and Löser, A. 2022. This patient looks like that patient: Prototypical networks for interpretable diagnosis prediction from clinical text. *arXiv preprint arXiv:2210.08500*.

Vu, T.; Nguyen, D. Q.; and Nguyen, A. 2020. A label attention model for ICD coding from clinical text. *arXiv preprint arXiv:2007.06351*.

Wang, T.; Zhang, L.; Ye, C.; Liu, J.; and Zhou, D. 2022. A novel framework based on medical concept driven attention for explainable medical code prediction via external knowledge. In *Findings of the Association for Computational Linguistics: ACL 2022*, 1407–1416.

Yang, X.; Bian, J.; Hogan, W. R.; and Wu, Y. 2020. Clinical concept extraction using transformers. *Journal of the American Medical Informatics Association*, 27(12): 1935–1942.

Yang, Z.; Wang, S.; Rawat, B. P. S.; Mitra, A.; and Yu, H. 2022. Knowledge injected prompt based fine-tuning for multi-label few-shot icd coding. In *Proceedings of the conference on empirical methods in natural language processing. Conference on empirical methods in natural language processing*, volume 2022, 1767.

Yogarajan, V.; Pfahringer, B.; Smith, T.; and Montiel, J. 2022. Concatenating BioMed-Transformers to Tackle Long Medical Documents and to Improve the Prediction of Tail-End Labels. In *International Conference on Artificial Neural Networks*, 209–221. Springer.

Yuan, Q.; Chen, J.; Lu, C.; and Huang, H. 2021. The graph-based mutual attentive network for automatic diagnosis. In *Proceedings of the Twenty-Ninth International Conference on International Joint Conferences on Artificial Intelligence*, 3393–3399.

Yuan, Z.; Tan, C.; and Huang, S. 2022. Code synonyms do matter: Multiple synonyms matching network for automatic ICD coding. *arXiv preprint arXiv:2203.01515*.

## A. Additional Information on Datasets and Implementation

### Datasets

**MIMIC Datasets** The Medical Information Mart for Intensive Care (MIMIC) dataset is a large-scale, de-identified database comprising health records of patients admitted to the emergency department or intensive care units at the Beth Israel Deaconess Medical Center (Johnson et al. 2020). The MIMIC-IV dataset covers over 65,000 ICU admissions

and more than 200,000 emergency department visits between 2008 and 2019, coded using ICD-10. The MIMIC-III dataset covers admissions between 2001 and 2012, including 52,723 discharge summaries from 41,126 patients, coded using ICD-9. Table 5 presents the statistics of dataset splits for all datasets used in model training, where “Ra” refers to the subset of data comprising documents with rationale labels generated by Gemini 2-Flash and it is used for training the multi-objective learning model. Top-50 subsets include only the 50 most frequent codes from the respective Full datasets.

Table 5: Dataset Split.

Dataset	Train	Test	Dev
MIMIC-IV ICD-10 Full	88988	19931	13360
MIMIC-IV ICD-10 Top-50	83890	18776	12590
MIMIC-III ICD-9 Full	47719	3372	1631
MIMIC-III ICD-9 Top-50	8066	1729	1573
MIMIC-IV ICD-10 Top-50 Ra	83465	18665	12517

**Entity Linking Dataset** The SNOMED CT Entity Linking Challenge dataset (Hardman et al. 2023) comprises 272 discharge summaries from MIMIC-IV-Note, annotated with 6,624 unique SNOMED-CT concepts. Among these, 64 documents overlap with the MIMIC-IV ICD-10 dataset. To enable comparison, we align SNOMED CT concepts with ICD-10 codes using established mapping resource (SNOMED-CT 2024).

### Implementation Details

**On CAML, LAAT and PLM-ICD** To ensure a fair comparison between models, we follow the experimental setup of Edin et al. (2023), which provides a reproducibility framework for state-of-the-art ICD coding models. Details of the key parameter configurations for the three ICD coding models are summarized in Table 5. All models are trained for 20 epochs, although CAML and LAAT typically converge within 10 epochs on MIMIC-IV ICD-10 and both MIMIC-III datasets. The random seed is set to 1337 for all model training.

**On Evaluation** During the faithfulness testing, if the whole document contains fewer than the threshold  $N$  tokens, we include all tokens. To evaluate comprehensiveness, if all tokens are removed, the single token with the lowest attention weight is retained.

**On NER** We implement the NER models using the default hyperparameter settings provided by Yang et al. (2020), with the parameter configuration summarized in Table 6. All NER models are trained on 5,000 randomly selected samples from the MIMIC-IV Top-50 dataset. Document-level plausibility evaluation is conducted on 139 annotated documents, filtered from an initial set of 150 samples to retain only those associated with the Top-50 codes. For code-level plausibility evaluation, the test set consists of the remaining samples, excluding those 5 samples used as examples in few-shot prompting. The statistics of the original and test sets are shown in Table 7.

Table 5: Configurations of CAML, LAAT and PLM-ICD.

Parameter	MIMIC-IV ICD-10 Full	MIMIC-IV ICD-10 Top-50	MIMIC-III ICD-9 Full	MIMIC-III ICD-9 Top-50
<b>CAML</b>				
batch size	8	8	8	8
learning rate	$5 \times 10^{-3}$	$5 \times 10^{-3}$	$10^{-4}$	$10^{-4}$
weight decay	$10^{-3}$	$10^{-3}$	-	-
<b>LAAT</b>				
batch size	8	8	8	8
learning rate	$10^{-3}$	$10^{-3}$	$10^{-3}$	$10^{-3}$
weight decay	$10^{-3}$	$10^{-3}$	-	-
<b>PLM-ICD</b>				
batch size	16	16	8	8
learning rate	$5 \times 10^{-5}$	$5 \times 10^{-5}$	$5 \times 10^{-5}$	$5 \times 10^{-5}$
weight decay	0	0	-	-

Table 6: Configurations of NER models.

Parameter	Value
batch size	8
learning rate	$10^{-5}$
warmup ratio	0.01
truncation	256
gradient accumulation steps	1
epoch	20
random seed	13

Table 7: Statistics of the test sets used for evaluating code-level NER models.

Code	Test Set / Full Set
I10	55 / 60
E785	50 / 55
Z7901	17 / 22
I4891	11 / 16
E119	17 / 22

## B. On LLM-Generated Rationales

### Prompting Without Examples

The used prompt without examples follows the format below. In the following, the *text*, *code*, and *description of the code* are variables that change based on the input note and the target code.

Note Text: *text* + Code: *code*. Description: *description of the code*. Could you please select the spans (rationales) which are related to the code *code*? The spans can be words, phrases, or sentences. Only list the exact spans extracted from the ‘Note Text’, without including their section names. List each span with a number in front. For example: ‘1. Span1 2. Span2’. Only keep the spans. Do not include any additional responses. Exclude any punctuations at the end of the spans. Keep the spans as what they are in ‘Note Text’. Keep the spans as what they are in ‘Note Text’. Keep the spans as what they are in the ‘Note Text’.

### Prompting With Few-Shot Examples

The used prompt with examples follows the format below. In the following, the variable *examples* represents annotation examples corresponding to each *code*.

Note Text: *text* + Code: *code*. Description: *description of the code*. Could you please select the spans (rationales) which are related to the code *code*? The spans can be words, phrases, or sentences. Only list the exact spans extracted from the ‘Note Text’, without including their section names. For example: *examples*. List each span with a number in front. For example: ‘1. Span1 2. Span2’. Only keep the spans. Do not include any additional responses. Exclude any punctuations at the end of the spans. Keep the spans as what they are in ‘Note Text’. Keep the spans as what they are in the ‘Note Text’. Keep the spans as what they are in the ‘Note Text’.

The examples are drawn from five randomly selected documents containing the given code in the annotation dataset. Table 8 summarizes the samples used for few-shot prompting and the corresponding *examples* value for each code.

### LLM Configurations

As the PhysioNet Credentialed Data Use Agreement prohibits sharing MIMIC data with external services such as ChatGPT, we follow PhysioNet’s recommendation to use Google Gemini, which does not utilize user prompts or responses for model training. We employ two variants of Gemini 2-Flash and 1.5-Pro. For local deployment, we select LLaMA-3.3, one of the most capable open-weight LLMs available, examining both the 70B Instruct and its quantized variant AWQ. The local LLMs are executed on  $4 \times$  and  $1 \times$  NVIDIA A100 80GB GPUs, respectively.

For the Gemini variants, we configured both models with a temperature of 0.1 to minimize randomness and encourage more deterministic outputs, as our task requires selecting spans that exactly match those appearing in the input documents. We also set top\_p to 0.99.

For the LLaMA variants, we adopted the same parameter settings as Gemini. Additionally, we set max\_tokens to 8,000, which exceeds the length of the longest documents in our dataset. This configuration, however, caused the computation for the larger LLaMA model to exceed the default

Code	Description	HADM IDs	Annotations
I10	Essential (primary) hypertension	21893270; 20961577; 20272030; 23048750; 29161744	'HTN', 'Hypertension', 'HYPERTENSION - ESSENTIAL, UNSPEC', 'Essential hypertension', 'hypertension', 'HYPERTENSION'
E785	Hyperlipidemia, unspecified	21893270; 26102343; 20272030; 24014389; 27049443	'HLD', 'Dyslipidemia', 'Hyperlipidemia', 'Hypercholesteremia', 'Dyslipidemia', 'hyperlipidemia'
Z7901	Long term (current) use of anticoagulants	27049443; 29964986; 27021287; 25097869; 29155448	'aspirin', 'Plavix', 'Coumadin', 'Afib on coumadin', "and the decision was made to restart the patient's ASA and Plavix immediately postoperatively", 'Clopidogrel 75 mg PO DAILY', 'Aspirin 325 mg PO DAILY', 'Warfarin', 'on Coumadi', 'Coumadin who presents with dyspnea', 'on coumadin', 'Warfarin held for supratherapeutic INR (INR 3.4)', 'afib on warfarin', 'On coumadin.', 'Warfarin 2 mg PO 1X/WEEK', 'Warfarin 5 mg PO 6X/WEEK', 'Warfarin 2 mg PO 1X/WEEK', 'on high-dose warfarin due to resistance', 'warfarin (5 mg)', 'heparin gtt', 'Aspirin 81 mg PO DAILY', 'Enoxaparin Sodium 140 mg', 'Aspirin 81 mg PO DAILY'
I4891	Unspecified atrial fibrillation	27049443; 24257587; 29964986; 27466246; 29588477	'atrial fibrillation', 'atrial fibrillation', 'Troponinemia', 'Atrial Fibrillation', 'Digoxin', 'afib', 'Afib on coumadin', 'afib s/p', 'Atrial fibrillation', 'Afib s/p ablation', 'Afib'
E119	Type 2 diabetes mellitus without complications	21893270; 27904530; 24257587; 25097869; 22473872	'diabetes', 'DM', 'Diabetes', 'DM2', 'BLOOD Glucose-113', 'Additionally, Diabetes service was consulted for newly found hyperglycemia.', 'insulin dependent DM', 'Diabetes: his hemoglobin A1c was 7.8.', 'type 2 diabetes mellitus'

Table 8: Samples used for few-shot prompting and their annotations.

memory capacity of two NVIDIA A100 80GB GPUs.

### Span Alignment for Rationale Generation

LLMs occasionally fail to consistently reproduce spans that exactly match those in the original patient notes, despite our explicit instruction emphasized in the prompt ‘*Keep the spans as they appear in the ‘Note Text’.*’ During the prompt engineering, we observe that repeating this instruction three times improve the consistency to some extent, but the generated spans are still not perfectly aligned. To address this issue and enable accurate evaluation against human annotations afterwards, we developed a post-processing method to map the LLM-generated spans back to the original text. Specifically, we first identify all candidate spans. We narrow the search window within the original text and extract all spans that share the same initial and terminal  $n$  characters as the generated rationale. We then compute their overlap scores to select the best match.

**Overlap Score Calculation** Let  $S_g$  and  $S_c$  be the generated rationale and candidate target span extracted from the document, respectively.  $T_g = \text{Tokenize}(S_g)$ , and  $T_c = \text{Tokenize}(S_c)$ , where  $\text{Tokenize}$  returns a set of tokens. The overlap score  $S$  is calculated by the following equation:

$$S = \frac{|T_g \cap T_c|}{|T_g|} + \frac{|T_g \cap T_c|}{|T_c|} \quad (3)$$

We present in Table 5 an example of overlap score calculation for a set of candidate spans corresponding to the generated span ‘*diagnosis type 2 diabetes*’, which shares the same initial character ‘d’ and terminal character ‘s’ (with a character window size of  $n = 1$ ). The overlap score consists of two components: (1) the overlap ratio with the generated rationale, which captures the degree of alignment with the generated rationale (e.g., ‘*diagnosis type 2 diabetes*’ (1) is preferred over ‘*diagnosis diabetes*’ (0.5)), and (2) the overlap ratio with the candidate span, which reflects the degree of alignment with the candidate span in the original text (e.g., ‘*diagnosis diabetes*’ (1) is preferred over ‘*diagnosis tuberculosis*’ (0.25)).

Table 5: Candidates targets of a generated rationale **diagnosis type 2 diabetes**. The decomposition consists of the two components of the overlap score function.

Candidate	Decomposition	Overlap Score
diagnosis	0.25 + 1	1.25
diabetes	0.25 + 1	1.25
diagnosis tuberculosis	0.25 + 0.5	0.75
dyslipidemias	0 + 0	0
diagnosis diabetes	0.5 + 1	1.5
diagnosis type 2 diabetes	1 + 1	2

**Rationale Selection** We repeat this process across a range of character window sizes and select the candidate with the highest overlap score as the final mapping result. This procedure is applied to all generated spans, and those with an

overlap score exceeding 1.7 are retained as supporting rationale for the document. The detailed steps of this mapping process are provided in the accompanying pseudocodes.

### C. More Details on Dataset Construction

**Data Selection** To build a comprehensive comparison that includes Entity Linking data, we first identify the overlap between the Entity Linking and the MIMIC-IV ICD-10 datasets. There are 64 overlapping samples between the two datasets. We then randomly select an additional 86 samples from the MIMIC-IV ICD-10 test set, resulting in a final dataset of 150 samples.

**Annotator** Two annotators with medical background contributed to this annotation work. One person annotated all samples (Annotator 1), while the other performed a quality check by annotating a subset of codes in 13 samples (Annotator 2).

**Annotation Guidelines** In this subsection, we outline the guidelines developed for the annotators.

*Title.* Identifying Rationales of ICD Codes in Discharge Summaries

*Purpose.* Explainability is especially critical in the clinical domain, where transparent and well-supported rationales enable healthcare providers and decision-makers to confidently utilize model predictions in patient care. The data you annotate will serve as a gold standard for evaluating the explainability of ICD coding models. By comparing rationales identified by these models with those provided by human annotators, we aim to assess how effectively the models present rationales, particularly in a human-understandable manner.

*Task Description.* In this task, you will be presented with a patient’s discharge summary and its assigned ICD (International Classification of Diseases) codes. Your goal is to identify and highlight text spans that support the given ICD codes as rationales. These highlighted spans may be words, phrases, or sentences (complete or incomplete).

*Platform Setup.*

- Install Docker following the official installation guide.
- Set up the annotation platform (Doccano).

*Annotation Process.*

- On the Doccano interface, you will see a patient’s discharge summary along with its assigned ICD-10 codes and their descriptions.
- As you review the summary, highlight all text spans that you believe support each label (ICD code).
- When you select a span with your mouse, a selection list will appear. Click the appropriate label to annotate the span with it. The same text span can be annotated with multiple labels.

*Completing the Annotation.*

- When you would like to save your current annotations, click the ‘X’ mark on the top left corner to change the status from ‘Not Checked’ to ‘Checked’.
- Once you have finished annotating all the labels for a summary, the sample will be marked as ‘Finished’.

---

**Algorithm 1: OverlapScore: Compute Overlap Score Between Two Spans**

---

**Input:** Generated span *generated\_span*, Candidate span *candidate\_span*

**Output:** Overlap score between the two spans

```
1:  $T_g \leftarrow \text{Tokenize}(\text{generated\_span})$ 
2:  $T_t \leftarrow \text{Tokenize}(\text{candidate\_span})$ 
3:  $I \leftarrow T_g \cap T_t$ 
4:  $\text{score} \leftarrow \frac{|I|}{|T_g|} + \frac{|I|}{|T_t|}$ 
5: return score
6: Notes: Tokenize function splits a text span into individual tokens.
```

---

---

**Algorithm 2: BestCandidate: Find Best Matching Candidate Span**

---

**Input:** Generated span *generated\_span*, Document *note*

**Output:** Best candidate and its overlap score

```
1: best_candidate  $\leftarrow ''$ 
2: max_score  $\leftarrow 0$ 
3: candidates  $\leftarrow []$ 
4: for  $n = 7$  to  $1$  step  $-1$  do
5:   span_start  $\leftarrow \text{Lower}(\text{generated\_span}[n])$ 
6:   span_end  $\leftarrow \text{Lower}(\text{generated\_span}[-n])$ 
7:   for  $i = 0$  to  $\text{Len}(\text{note}) - n$  do
8:     window_start  $\leftarrow \text{Lower}(\text{note}[i:i+n])$ 
9:     if window_start  $==$  span_start then
10:      start_index  $\leftarrow i$ 
11:      for  $j = 0$  to  $\text{Len}(\text{note}) - \text{start\_index} - n$  do
12:        end_index  $\leftarrow \text{Len}(\text{note}) - j$ 
13:        if end_index  $- n < 0$  then
14:          break
15:        end if
16:        window_end  $\leftarrow \text{Lower}(\text{note}[\text{end\_index} - n : \text{end\_index}])$ 
17:        if window_end  $==$  span_end and end_index  $>$  start_index then
18:          text_candidate  $\leftarrow \text{note}[\text{start\_index} : \text{end\_index}]$ 
19:          candidates  $\leftarrow \text{candidates} \cup \text{text\_candidate}$ 
20:        end if
21:      end for
22:    end if
23:  end for
24: end for
25: for item in candidates do
26:   score  $\leftarrow \text{OverlapScore}(\text{generated\_span}, \text{item})$ 
27:   if score  $>$  max_score then
28:     max_score  $\leftarrow \text{score}$ 
29:     best_candidate  $\leftarrow \text{item}$ 
30:   end if
31: end for
32: return best_candidate, max_score
33: Notes: Lower denotes the lowercase conversion function; Len function returns the length of a string.
```

---



**Platform** We conducted the annotation using Doccano, a free and open-source platform designed to facilitate the creation of labeled datasets for natural language processing tasks. Doccano supports various annotation types, including text classification, sequence labeling (e.g., named entity recognition), and sequence-to-sequence tasks (e.g., machine translation or summarization). For this study, we employ the sequence labeling functionality. In the setup, the ‘Allow overlapping spans’ and ‘Share annotations across all users’ options are enabled. Additionally, a separate project is created for each document, each with its own defined label set.

**Inter-Annotator Agreement** Inter-annotator agreement (IAA) refers to the degree of consistency or reliability among different human annotators who independently annotate the same dataset. It is a critical measure to assess the quality and objectivity of annotated data, especially in tasks involving subjective judgments. We evaluate the annotation quality through a secondary annotator, who annotate the rationales for a subset of codes across 13 samples. To assess agreement, we calculate both span-level and token-level matching scores, including Precision, Recall and F1.

Here we explain how these scores are computed. Let  $A_2$  be the set of tokens annotated by Annotator 2 and  $A_1$  be the set of tokens annotated by Annotator 1. The overlap between these sets is:

$$\text{Overlap} = A_2 \cap A_1. \quad (4)$$

Precision, recall, and F1 scores are computed as follows:

$$\text{Precision} = \frac{|A_2 \cap A_1|}{|A_1|}, \quad (5)$$

$$\text{Recall} = \frac{|A_2 \cap A_1|}{|A_2|}, \quad (6)$$

$$\text{F1} = 2 \times \frac{\text{Precision} \times \text{Recall}}{\text{Precision} + \text{Recall}}. \quad (7)$$

Table 6 presents the results of the inter-annotator agreement analysis. The token-level F1-score (53.32) is substantially higher than the span-level F1-score (31.58), indicating that annotators exhibit greater consistency in identifying relevant content than in determining precise span boundaries. Table 7 provides a subset of detailed annotation matches between the two annotators.

Table 6: Inter-Annotator Agreement

Metric	Value (%)
Span-Level Precision	38.00
Span-Level Recall	30.95
Span-Level F1	31.58
Token-Level Precision	79.84
Token-Level Recall	44.16
Token-Level F1	53.32

**ICD Codes with no supporting evidence** During the annotation, we observe that not all codes have their supporting rationales in the text. This also serves the analysis of the quality of the MIMIC-IV ICD10 dataset. We list all codes with no rationale in Table 8.

**Details of Data Processing** When evaluating plausibility, the original rationale annotations are preprocessed to align with the input formats of ICD coding models. We apply the same preprocessing procedures used in Edin et al. (2023)’s medical coding reproducibility study. Specifically, CAML and LAAT annotations are cleaned by lowercasing, removing special characters and stray numbers, and trimming extra spaces. For PLM-ICD, this cleaning step is followed by tokenization using the RoBERTa-base-PM-M3-Voc-distill-align-hf tokenizer from Hugging Face. These procedures ensure that the rationales extracted by each model are accurately comparable to our processed gold-standard annotations.

## D. Code Overlap Analysis: MDACE and MIMIC-III ICD-9

MDACE annotates a subset of MIMIC-III clinical notes with ICD-10 codes and their corresponding rationales, which are then automatically mapped to ICD-9 codes using the General Equivalence Mappings (GEMs). This mapping introduces inconsistencies with the original ICD-9 code distribution in the MIMIC-III dataset commonly used for ICD coding tasks. We analyze the overlap between the two datasets under both the *Full* code setting and the *Top-50* code setting, with average overlaps of 37.00% and 14.59%, respectively. Figure 6 presents the distribution of overlap ratios in terms of number of documents and cumulative proportion. The results indicate that, for approximately 80% of the documents, the code overlap is below 60%. In the Top-50 setting, none of the documents exhibit more than 60% overlap. Figure 7 presents the frequency distribution of the Top-50 ICD-9 codes in both MDACE and the original MIMIC-III ICD-9 dataset. Notably, 6 of the Top-50 codes are entirely missing in MDACE (and 725 codes are missing in the Full-code setting, which comprises 1,281 codes in total). This substantial inconsistency poses challenges in accurately evaluating the explainability of ICD coding models.

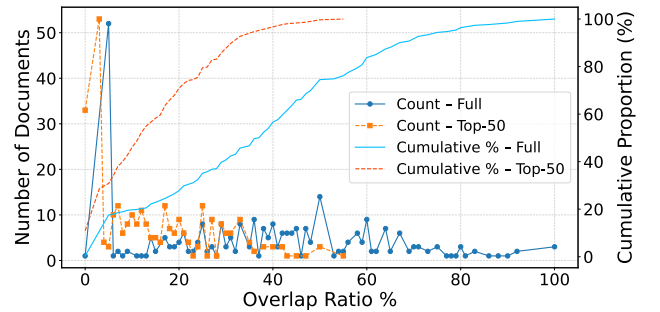


Figure 6: The statistics of overlap between MIMIC-III ICD-9 code set and mapped ICD-9 code set in MDACE.

## E. A Case Study: Comparing Annotation Quality in RD-IV-10 and MDACE

Table 1 indicates that, on average, each ICD code in MDACE is associated with roughly one supporting ratio-

HADM ID	Code	Annotator2	Annotator1	Match
29531980	027034Z	'Left heart cath'	'nan'	False
29531980	I10	'hypertension'	'hypertension'	True
29531980	E1140	'type 2 diabetes'	'type 2 diabetes'	True
29531980	N390	'MRSA UTI'	'MRSA UTI'	False
29531980	E1140	'Diabetes'	'Diabetes'	True
29531980	I10	'Hypertension'	'Hypertension'	True
29531980	I10	'Hypertension'	'Hypertension'	True
29531980	E1140	'Diabetes'	'Diabetes'	True
29531980	I10	'hypertension'	'hypertension'	True
29474957	W363XXA	'Trauma'	'nan'	False
29474957	W363XXA	'patient reports that he was blown off by the lid of a highly pressurized natural gas tank in his pickup truck and sustained multiple injuries from the blast'	'he was blown off by the lid of a highly pressurized natural gas tank in his pickup truck and sustained multiple injuries from the blast'	False
29474957	H05221	'Right periorbital soft tissue swelling '	'Right periorbital soft tissue swelling '	True
29474957	S2241XA	'Right-sided rib fractures'	'rib fractures '	False
29474957	S2241XA	'Right-sided rib fractures involving the eighth and ninth ribs which appear comminuted displaced as well as fractured right tenth rib at the costovertebral junction'	'Right-sided rib fractures involving the eighth and ninth ribs which appear comminuted displaced as well as fractured right tenth rib at the costovertebral junction. '	False

Table 7: Part of annotation details of two annotators.

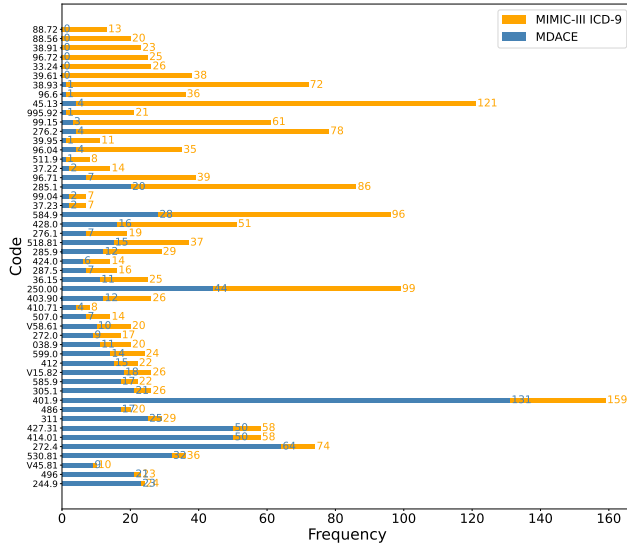


Figure 7: The frequency of codes in the code sets in MDACE and MIMIC-III ICD-9.

nale, given the ratio of 13.83 evidence spans to 11.53 labels per document. In contrast, RD-IV-10 provides substantially richer annotations, averaging 35.94 rationales for 14.82 labels per document. To illustrate this discrepancy, we present a case study shown in Figure 8 comparing both datasets. We randomly select one document annotated with the ICD-10 code **Z79.02 - Long-term use of antithrombotics/antiplatelets** from two datasets. In MDACE, the sole highlighted rationale is ‘*plavix 75 mg*’. RD-IV-10, however, highlights not only ‘*Plavix*’ but also other directly relevant medications such as ‘*aspirin*’ and ‘*clopidogrel*’, found in multiple locations that MDACE fails to capture (highlighted in grey in the visualization). Additionally, our dataset annotates indirect supportive evidence ‘*However, patient declined cardiac catheterization given his desire for no invasive procedures*’. This statement reinforces the patient’s complex cardiac history and justifies ongoing antiplatelet therapy, despite declining further interventions.

## F. Complete Results of Faithfulness and Plausibility of CAML, LAAT and PLM-ICD

**Results of Faithfulness** Tables 14, 15, and 16 summarize the faithfulness results of CAML, LAAT, and PLM-ICD, respectively, using two rationale selection strategies across four MIMIC datasets.

**Results of Plausibility** Tables 17, 18, and 19 summarize the plausibility results of CAML, LAAT, and PLM-ICD, respectively, using two rationale selection strategies across all threshold settings.

## G. Complete Results of Plausibility

**Plausibility Results of Three Types of Rationales** Table 9 presents the plausibility results of naive entity-level rationales, strong LLM-generated rationales, model-generated rationales.

HADM ID	ICD-10 Code
21843396	J45909;02HV33Z
29964986	30283B1;Z87891
29918504	F17210
29677969	Z96651;Z22322
28100046	J9811;J95811;Z23
27638102	F17290
27044834	E860
26620438	E8342
25912628	Z87891
24823574	Z87891
23856554	Z87891
23702445	F329
23355051	Z87891
23295582	Z87891;F419
29588477	02HV33Z
22893898	E874;J984;E870;H40052;Y848;Y92230;I9581;05UL0KZ;0NS60ZZ;08N1XZZ;02HV33Z
23051773	I25118;D62;D696;R350;5A1221Z
23618067	Z23
27840655	I5033;I110
22528733	N814
23106502	I082;I671;H409;R6884;Z87891;Y92009
25920183	A549;02HV33Z
26094695	Z66;R627;Z6821
27356906	J9600;Z781;K7290;Z87891;06L34CZ
21222006	Z22321
21318772	I2109;Z23;E861;R740;B1920
21386441	F17210
22257486	G4733
22733522	G4733;E669;Z6833;Z87891
23354056	D696;E860
23694175	K648;R29700
24345583	F17210
24852593	F0390;Z86711
25307585	E881;A630;L732;Z87891
25334768	A419;E46;I272
25510774	F1021
26911900	Z9119
27567712	T859XXA;T81.4XXA;Y92129;Z85820;0FPGX0Z;0F2GX0Z;02HV33Z;0JD80ZZ;0DHA8UZ;3E0H76Z
28716988	Z781
28831703	T8172XA;I808
29520101	Z87891
22032290	K55029;R6521;D62;F05;Z66;F17210
22114206	Z87891
22556702	Z006;K219
22983901	D6832;D6959;Z87891;T45515A
23383624	M25561;Z87820
23869666	E46;Z6829
24309140	B9562;I452;Z8673;Z86711;F17210;0W383ZZ;02H633Z
24352758	D684;N179;Z87891;D6959;Z781;0BC68ZZ;0BC48ZZ;3E0G76Z
24378932	N179;N182
24672299	Z87891
24974242	F17210
24991332	I871;05JY3ZZ
26852604	Z87891
27705753	Z87891;0U20KZ
28206965	I509;F05;BT11YZZ
28731328	Z87891;R0682;F40240
28756843	I959;Z87891
29060004	Z87891
29402217	Z22322

Table 8: Codes without supporting rationales in the document.

MDACE	HADM-ID: 112338
Admission Date: [**2189-1-29**] Discharge Date: [**2189-2-2**] Date of Birth: [**2116-1-21**] Sex: F ... Medications on Admission: plavix 75mg omeprazole 20mg [**Hospital1 **] ... zocor 40mg aspirin 81mg percocet amidarone 400mg lopressor 75mg Discharge Medications: 1. Clopidogrel 75 mg Tablet Sig: One (1) Tablet PO DAILY (Daily). Disp:*60 Tablet(s)* Refills:*0* 2. Omeprazole 20 mg Capsule, Delayed Release(E.C.) Sig: One (1) Capsule, Delayed Release(E.C.) PO BID (2 times a day). Disp:*60 Capsule, Delayed Release(E.C.)(s)* Refills:*0* 3. Docusate Sodium 100 mg Capsule Sig: One (1) Capsule PO BID (2 times a day). Disp:*60 Capsule(s)* Refills:*0* 4. Aspirin 81 mg Tablet, Chewable Sig: One (1) Tablet, Chewable PO DAILY (Daily). Disp:*60 Tablet, Chewable(s)* Refills:*0* 5. Oxycodone-Acetaminophen 5-325 mg Tablet Sig: 1-2 Tablets PO Q6H (every 6 hours) as needed. Disp:*40 Tablet(s)* Refills:*0* ... [**Name6 (MD) **] [**Name8 (MD) **] MD [**MD Number(2) 173**] Completed by:[**2189-2-2**]	
RD-IV-10	HADM-ID: 27638102
Name: ____ Unit No: ____ Admission Date: ____ Discharge Date: ____ Date of Birth: ____ Sex: M ... Brief Hospital Course: Mr. ____ is an ____ yo man with a history of NSTEMI s/p s/p DES to LAD (____), LCX (____) who presented with right sided light chest pressure at rest which was similar to his previous NSTEMIs. Of note, he described holding his aspirin and clopidogrel for a Dermatology procedure. ACTIVE PROBLEMS # NSTEMI # Community acquired pneumonia He was noted to have an NSTEMI with troponins peaking at 0.03. His EKG was unremarkable for ischemic change, normal sinus rhythm, TWI in V1, no STE, unchanged from prior. He was placed on a heparin gtt with a plan for cardiac catheterization. However, patient declined cardiac catheterization given his desire for no invasive procedures. He also declines reversal of code status from DNR/DNI for procedures. He is on Plavix, aspirin, carvidiolol, atorvastatin 80, and lisinopril-HCTZ at home, and these were continued. Also, we counseled the patient yesterday that he could NOT, under any circumstances, discontinue his DAPT without a cardiologist's permission. ... Medications on Admission: The Preadmission Medication list is accurate and complete. 1. Amlodipine 10 mg PO DAILY 2. Aspirin 81 mg PO DAILY 3. BuPROPion (Sustained Release) 300 mg PO QAM 4. Clopidogrel 75 mg PO DAILY 5. DiphenhydrAMINE 25 mg PO QHS insomnia ... Discharge Medications: 1. Amlodipine 10 mg PO DAILY 2. Amphetamine-Dextroamphetamine 10 mg PO TID 3. Aspirin 81 mg PO DAILY 4. Atorvastatin 80 mg PO QPM 5. BuPROPion (Sustained Release) 300 mg PO QAM 6. Clopidogrel 75 mg PO DAILY 7. DiphenhydrAMINE 25 mg PO QHS insomnia 8. Fluticasone Propionate NASAL 2 SPRY NU DAILY PRN 9. Lorazepam 1.5 mg PO QHS insomnia 10. Multivitamins 1 TAB PO DAILY ... Your ____ team Followup Instructions: ____	

Figure 8: A case study of the annotation quality of RD-IV-10 and MDACE.

Metric	Model/Dataset	Prdiction	Accurate	TP	FP	FN	Precision (%)	Recall (%)	F1 (%)
Exact SM	Entity-Linking	3546	2260	298	3248	1962	8.4	13.2	10.3
	Gemini 2-Flash	4726	2260	754	3972	1506	16.0	33.4	21.6
	Gemini1.5-Pro	11184	2260	907	10277	1353	8.1	40.1	13.5
	LLaMA-3.3 Ins	5789	2260	747	5042	1513	12.9	33.1	18.6
	LLaMA-3.3 AWQ	6428	2260	761	5667	1499	11.8	33.7	17.5
	CAML	84520	2269	55	84465	2214	0.1	2.4	0.1
	LAAT	91482	2269	330	91152	1939	0.4	14.5	0.7
	PLM-ICD	65639	2269	172	65467	2097	0.3	7.6	0.5
PI SM	Entity-Linking	2751	1762	207	2544	1555	7.5	11.7	9.2
	Gemini-2flash	4664	1762	773	3891	989	16.6	43.9	24.1
	Gemini-1.5pro	10996	1762	932	10064	830	8.5	52.9	14.6
	LLaMA-3.3 Ins	5726	1762	805	4921	957	14.1	45.7	21.5
	LLaMA-3.3 AWQ	6364	1762	816	5548	946	12.8	46.3	20.1
	CAML	77970	2021	88	77882	1933	0.1	4.4	0.2
	LAAT	82542	2021	342	82200	1679	0.4	16.9	0.8
	PLM-ICD	60851	2041	228	60623	1813	0.4	11.2	0.7
Exact TM	Entity-Linking	5629	11422	540	5089	10882	9.6	4.7	6.3
	Gemini-2flash	27639	11422	5881	21758	5541	21.3	51.5	30.1
	Gemini-1.5pro	57708	11422	7109	50599	4313	12.3	62.2	20.6
	LLaMA-3.3 Ins	28800	11422	5588	23212	5834	19.4	48.9	27.8
	LLaMA-3.3 AWQ	32693	11422	6008	26685	5414	18.4	52.6	27.2
	CAML	150968	11428	2493	148475	8935	1.7	21.8	3.1
	LAAT	160732	11428	4266	156466	7162	2.7	37.3	5.0
	PLM-ICD	173633	12517	3975	169658	8542	2.3	31.8	4.3
PI TM	Entity-Linking	4292	8160	381	3911	7779	8.9	4.7	6.1
	Gemini-2flash	18935	8160	5047	13888	3113	26.7	61.9	37.3
	Gemini-1.5pro	37197	8160	5898	31299	2262	15.9	72.3	26.0
	LLaMA-3.3 Ins	20708	8160	5056	15652	3104	24.4	62.0	35.0
	LLaMA-3.3 AWQ	23302	8160	5361	17941	2799	23.0	65.7	34.1
	CAML	114766	9367	4029	110737	5338	3.5	43.0	6.5
	LAAT	121292	9367	4720	116572	4647	3.9	50.4	7.2
	PLM-ICD	120777	10269	5794	114983	4475	4.8	56.4	8.8

Table 9: Plausibility results of **naive entity-level rationales**, **strong LLM-generated rationales**, **model-generated rationales (no supervision)**. Prediction refers to the number of spans or tokens generated by the model, while Accurate denotes the number of spans or tokens matching the human-annotated gold standard. This evaluation is based on 64 documents to enable a comparison of entity linking.



**Plausibility Results of Top 5 Codes (Rationales Generated by Gemini 2-Flash)** Table 10 summarizes the plausibility results of top 5 codes with and without incorporating few-shot human-annotated examples in the prompts. Incorporating few-shot examples substantially improves performance across all five codes and metrics. Notably, the token-level matches for I10 and the span-level matches for I4891 nearly double compared to those generated without few-shot examples.

**Plausibility Results of LLMs-guided Rationale Learning Approaches** Table 11 presents the plausibility results of the multi-objective model and its base model, PLM-ICD. We compare their performance across different numbers of selected tokens, ranging from 50 to 200. The multi-objective model consistently outperforms the base model across all settings and metrics, with particularly notable gains in span-level matches. Interestingly, the improvements are more pronounced at lower thresholds, indicating that the model generates more concise rationales, whereas at higher thresholds the performance gap narrows as more tokens are incorporated.

Table 12 presents the plausibility results of the NER model trained on a small dataset of 5,000 randomly selected samples. The results show that the NER model achieves the highest span-level plausibility, even surpassing its teacher model, Gemini 2-Flash. In contrast, PLM-ICD performs the worst. Interestingly, training on the smaller dataset improves plausibility compared to the results in Table 11. We attribute this finding to the influence of rationale proportions on the model’s ability to generate plausible rationales.

**Plausibility Results of Top 5 Codes (Rationales Generated by NER with Supervision of Rationales Labels Generated by Gemini 2-Flash)** Table 13 presents the plausibility results for the top 5 codes. The rationales are generated using NER models trained on rationales produced by Gemini 2-Flash, with and without the inclusion of few-shot human-annotated examples in the prompts. Models incorporating few-shot examples demonstrate improved performance across most codes and metrics. Furthermore, the supervised model outperforms the unsupervised model for codes I10, E785, and E119, due to the higher frequency of corresponding rationales in the documents.

## H. A Case Study: Comparative Analysis of Rationales From Four Sources

To examine the rationales produced by different sources in detail, we present a case study comparing Human Annotation, Entity-Linking, Gemini 2-Flash, and PLM-ICD. The focus is on rationales for ICD-10 code N49.2 – Inflammatory disorders of scrotum. We randomly select the document HADM-ID 29964986, to illustrate how each method justifies the assigned code.

Table 9 shows that Entity Linking and Human Annotation partially overlap. Entity Linking highlights only the direct mentions of the code, such as ‘SCROTAL’ and ‘scrotal abscess’, whereas Human Annotation additionally mark broader contextual information—the sentence: ‘This patient

was admitted to the urology service following debridement of scrotal and perineal abscess.’ Gemini 2-Flash also performs well in this case. It highlights phrases overlooked by both human annotators and Entity Linking—such as ‘scrotal and perineal abscess’ and ‘right scrotal fluctuance’—and even captures parts of that human-annotated sentence. However, it also returns some incorrect spans, including ‘Perineal abscess’ and ‘Hemiscrotum’. Additionally, we observe that the rationales of PLM-ICD are randomly distributed and lack meaningful explainability; therefore, we do not visualize them in this case study. This case study supports our earlier conclusion that Gemini 2-Flash achieves the highest plausibility, while naive directly linked entities can also serve as rationales to a certain extent. In contrast, the rationales generated by PLM-ICD exhibit the lowest plausibility.

Code	Metric	Setting	Prdiction	Accuturate	TP	FP	FN	Precision (%)	Recall (%)	F1 (%)	$\Delta F1$
I10	Exact SM	w/o	147	151	75	72	76	51.0	49.7	50.3	+10.2
		w/	107	141	75	32	66	70.1	53.2	60.5	
	PI SM	w/o	140	82	70	70	12	50.0	85.4	63.1	+15.1
		w/	100	79	70	30	9	70.0	88.6	78.2	
	Exact TM	w/o	526	155	92	434	63	17.5	59.4	27.0	+26.8
		w/	182	145	88	94	57	48.4	60.7	53.8	
	PI TM	w/o	411	86	80	331	6	19.5	93.0	32.2	+34.2
		w/	152	83	78	74	5	51.3	94.0	66.4	
E785	Exact SM	w/o	79	97	55	24	42	69.6	56.7	62.5	+10.7
		w/	69	95	60	9	35	87.0	63.2	73.2	
	PI SM	w/o	72	56	49	23	7	68.1	87.5	76.6	+12.9
		w/	60	54	51	9	3	85.0	94.4	89.5	
	Exact TM	w/o	140	107	62	78	45	44.3	57.9	50.2	+16.5
		w/	84	99	61	23	38	72.6	61.6	66.7	
	PI TM	w/o	125	66	57	68	9	45.6	86.4	59.7	+18.5
		w/	75	58	52	23	6	69.3	89.7	78.2	
Z7901	Exact SM	w/o	83	50	6	77	44	7.2	12.0	9.0	+4.0
		w/	102	52	10	92	42	9.8	19.2	13.0	
	PI SM	w/o	82	42	6	76	36	7.3	14.3	9.7	+7.1
		w/	100	43	12	88	31	12.0	27.9	16.8	
	Exact TM	w/o	524	387	163	361	224	31.1	42.1	35.8	+10.0
		w/	645	389	237	408	152	36.7	60.9	45.8	
	PI TM	w/o	354	265	134	220	131	37.9	50.6	43.3	+11.5
		w/	413	266	186	227	80	45.0	69.9	54.8	
I4891	Exact SM	w/o	47	55	6	41	49	12.8	10.9	11.8	+12.9
		w/	42	55	12	30	43	28.6	21.8	24.7	
	PI SM	w/o	45	27	6	39	21	13.3	22.2	16.7	+20.2
		w/	38	27	12	26	15	31.6	44.4	36.9	
	Exact TM	w/o	221	93	44	177	49	19.9	47.3	28.0	+19.9
		w/	124	93	52	72	41	41.9	55.9	47.9	
	PI TM	w/o	164	37	35	129	2	21.3	94.6	34.8	+21.4
		w/	84	37	34	50	3	40.5	91.9	56.2	
E119	Exact SM	w/o	53	50	21	32	29	39.6	42.0	40.8	+3.4
		w/	54	50	23	31	27	42.6	46.0	44.2	
	PI SM	w/o	53	33	21	32	12	39.6	63.6	48.8	+4.1
		w/	54	33	23	31	10	42.6	69.7	52.9	
	Exact TM	w/o	225	79	55	170	24	24.4	69.6	36.2	+7.4
		w/	187	79	58	129	21	31.0	73.4	43.6	
	PI TM	w/o	186	49	44	142	5	23.7	89.8	37.4	+7.4
		w/	152	49	45	107	4	29.6	91.8	44.8	

Table 10: Plausibility results of top 5 codes. Rationales are generated by Gemini 2-Flash. “w/o” and “w/” indicate the absence or inclusion of few-shot examples in prompts.

Setting	Model	Exact Span			PI Span			Exact Token			PI Token		
		Pr	Rc	F1	Pr	Rc	F1	Pr	Rc	F1	Pr	Rc	F1
50	PLM-ICD	1.5	14.2	2.7	1.7	17.2	3.0	5.5	35.1	9.5	7.1	43.8	12.2
	Multi-objective	2.1	20.9	3.9	2.2	23.5	4.1	6.1	39.1	10.6	7.6	47.4	13.2
100	PLM-ICD	0.6	9.3	1.1	0.7	11.8	1.3	2.9	36.9	5.5	4.5	51.7	8.3
	Multi-objective	1.0	16.6	1.9	1.1	18.8	2.0	3.2	40.2	5.9	4.7	53.5	8.6
150	PLM-ICD	0.3	7.1	0.6	0.4	10.0	0.8	2.0	37.4	3.8	3.5	56.9	6.6
	Multi-objective	0.7	14.0	1.3	0.8	16.9	1.4	2.1	38.2	3.9	3.5	55.2	6.5
200	PLM-ICD	0.2	6.6	0.5	0.3	9.7	0.7	1.5	36.2	2.8	2.9	59.9	5.6
	Multi-objective	0.5	12.4	1.0	0.6	14.9	1.1	1.6	38.4	3.0	2.9	58.8	5.5

Table 11: Plausibility results of multi-objective learning approach and the baseline model PLM-ICD. All results are reported as percentages. The experiments are conducted under the Top-50 code settings.

Setting	Model	Exact Span			PI Span			Exact Token			PI Token		
		Pr	Rc	F1	Pr	Rc	F1	Pr	Rc	F1	Pr	Rc	F1
-	NER Model	29.3	24.3	26.5	29.0	32.5	30.6	35.1	15.8	21.8	37.1	21.2	27.0
-	Gemini 2-Flash	16.4	20.5	18.2	18.2	31.2	23.0	23.0	40.6	29.4	23.7	46.4	31.4
50	PLM-ICD	2.5	12.8	4.1	2.5	14.8	4.3	4.7	28.2	8.1	7.0	41.6	12.0
100	PLM-ICD	1.5	11.9	2.6	1.6	14.3	2.8	2.7	31.5	4.9	4.7	51.2	8.7
150	PLM-ICD	0.9	9.7	1.7	1.0	12.6	1.9	1.9	33.0	3.5	3.7	56.4	6.9
200	PLM-ICD	0.6	7.5	1.1	0.7	10.0	1.3	1.5	35.1	2.9	3.1	60.5	6.0

Table 12: Plausibility results for the NER model, the teacher model Gemini 2-Flash, and the baseline model PLM-ICD. All results are reported as percentages. The experiments are conducted under the Top-50 code settings.

RD-IV-10	Entity Linking	Gemini 2-Flash
<p>Name: ____ Unit No: ____</p> <p>Admission Date: ____ Discharge Date: ____</p> <p>Date of Birth: ____ Sex: M</p> <p>Service: UROLOGY</p> <p>Allergies:</p> <p>ciprofloxacin</p> <p>Attending: ____</p> <p>Chief Complaint:</p> <p><b>SCROTAL/PERINEAL ABSCESS</b></p> <p>Major Surgical or Invasive Procedure:</p> <p>1. Exam under anesthesia.</p> <p>2. Debridement of scrotal and perineal abscess.</p> <p>History of Present Illness:</p> <p>...</p> <p>chronic indwelling Foley; transferred from ____ with <b>right scrotal abscess</b>.</p> <p>Patient presented to his see his urologist (____)</p> <p>...</p> <p>empiric treatment.</p> <p>When found to have right scrotal fluctuance, there was an ultrasound performed that showed <b>right scrotal abscess</b> with concern for fluid and gas extending into the</p> <p>...</p> <p>place; ____ wick removed. Hemiscrotum</p> <p>Incision c/d/i w/out</p> <p>...</p> <p>fluid should be submitted.</p> <p>Brief Hospital Course:</p> <p><b>This patient was admitted to the urology service following debridement of scrotal and perineal abscess.</b> See operative report for full details. The patient tolerated the procedure well and recovered in the PACU before transfer to the surgical floor. He was admitted on zosyn/clindamycin for antibiotic ...</p> <p>Discharge Diagnosis:</p> <p>PREOPERATIVE DIAGNOSES:</p> <p>1. <b>Scrotal abscess.</b></p> <p>2. Perineal abscess.</p> <p>POSTOPERATIVE DIAGNOSES:</p> <p>1. <b>Scrotal abscess.</b></p> <p>2. Perineal abscess.</p>	<p>Name: ____ Unit No: ____</p> <p>Admission Date: ____ Discharge Date: ____</p> <p>Date of Birth: ____ Sex: M</p> <p>Service: UROLOGY</p> <p>Allergies:</p> <p>ciprofloxacin</p> <p>Attending: ____</p> <p>Chief Complaint:</p> <p><b>SCROTAL /PERINEAL ABSCESS</b></p> <p>Major Surgical or Invasive Procedure:</p> <p>1. Exam under anesthesia.</p> <p>2. Debridement of scrotal and perineal abscess.</p> <p>History of Present Illness:</p> <p>...</p> <p>chronic indwelling Foley; transferred from ____ with right <b>scrotal abscess</b>.</p> <p>Patient presented to his see his urologist (____)</p> <p>...</p> <p>empiric treatment.</p> <p>When found to have right scrotal fluctuance, there was an ultrasound performed that showed right scrotal abscess with concern for fluid and gas extending into the</p> <p>...</p> <p>place; ____ wick removed. Hemiscrotum</p> <p>Incision c/d/i w/out</p> <p>...</p> <p>fluid should be submitted.</p> <p>Brief Hospital Course:</p> <p>This patient was admitted to the urology service following debridement of scrotal and perineal abscess. See operative report for full details. The patient tolerated the procedure well and recovered in the PACU before transfer to the surgical floor. He was admitted on zosyn/clindamycin for antibiotic ...</p> <p>Discharge Diagnosis:</p> <p>PREOPERATIVE DIAGNOSES:</p> <p><b>1. Scrotal abscess.</b></p> <p>2. Perineal abscess.</p> <p>POSTOPERATIVE DIAGNOSES:</p> <p>1. Scrotal abscess.</p> <p>2. Perineal abscess.</p>	<p>Name: ____ Unit No: ____</p> <p>Admission Date: ____ Discharge Date: ____</p> <p>Date of Birth: ____ Sex: M</p> <p>Service: UROLOGY</p> <p>Allergies:</p> <p>ciprofloxacin</p> <p>Attending: ____</p> <p>Chief Complaint:</p> <p><b>SCROTAL/PERINEAL ABSCESS</b></p> <p>Major Surgical or Invasive Procedure:</p> <p>1. Exam under anesthesia.</p> <p>2. Debridement of <b>scrotal and perineal abscess</b>.</p> <p>History of Present Illness:</p> <p>...</p> <p>chronic indwelling Foley; transferred from ____ with <b>right scrotal abscess</b>.</p> <p>Patient presented to his see his urologist (____)</p> <p>...</p> <p>empiric treatment.</p> <p>When found to have right scrotal fluctuance, there was an ultrasound performed that showed <b>right scrotal abscess</b> with concern for fluid and gas extending into the</p> <p>...</p> <p>place; ____ wick removed. <b>Hemiscrotum</b></p> <p>Incision c/d/i w/out</p> <p>...</p> <p>fluid should be submitted.</p> <p>Brief Hospital Course:</p> <p>This patient was admitted to the urology service following <b>debridement of scrotal and perineal abscess</b>. See operative report for full details. The patient tolerated the procedure well and recovered in the PACU before transfer to the surgical floor. He was admitted on zosyn/clindamycin for antibiotic ...</p> <p>Discharge Diagnosis:</p> <p>PREOPERATIVE DIAGNOSES:</p> <p>1. <b>Scrotal abscess.</b></p> <p>2. <b>Perineal abscess.</b></p> <p>POSTOPERATIVE DIAGNOSES:</p> <p>1. Scrotal abscess.</p> <p>2. Perineal abscess.</p>

Figure 9: A case study of annotations of RD-IV-10, Entity Linking and Gemini 2-Flash. The highlights indicate their corresponding annotations.

Code	Metric	Setting	Prdiction	Accturate	TP	FP	FN	Precision (%)	Recall (%)	F1 (%)	$\Delta F1$
I4891	Exact SM	w/o	44	55	11	33	44	25.0	20.0	22.2	+3.9
		w/	37	55	12	25	43	32.4	21.8	26.1	
	PI SM	w/o	42	27	13	29	14	31.0	48.1	37.7	+5.6
		w/	33	27	13	20	14	39.4	48.1	43.3	
	Exact TM	w/o	115	93	40	75	53	34.8	43.0	38.5	+2.2
		w/	89	93	37	52	56	41.6	39.8	40.7	
	PI TM	w/o	86	37	30	56	7	34.9	81.1	48.8	+5.7
		w/	62	37	27	35	10	43.5	73.0	54.5	
I10	Exact SM	w/o	80	144	62	18	82	77.5	43.1	55.4	+7.1
		w/	80	144	70	10	74	87.5	48.6	62.5	
	PI SM	w/o	74	82	60	14	22	81.1	73.2	76.9	+8.3
		w/	73	82	66	7	16	90.4	80.5	85.2	
	Exact TM	w/o	93	147	67	26	80	72.0	45.6	55.8	+9.1
		w/	84	147	75	9	72	89.3	51.0	64.9	
	PI TM	w/o	85	85	64	21	21	75.3	75.3	75.3	+10.9
		w/	75	85	69	6	16	92.0	81.2	86.2	
E785	Exact SM	w/o	62	103	56	6	47	90.3	54.4	67.9	+2.4
		w/	62	103	58	4	45	93.5	56.3	70.3	
	PI SM	w/o	56	61	50	6	11	89.3	82.0	85.5	+1.5
		w/	54	61	50	4	11	92.6	82.0	87.0	
	Exact TM	w/o	64	121	57	7	64	89.1	47.1	61.6	+1.4
		w/	63	121	58	5	63	92.1	47.9	63.0	
	PI TM	w/o	57	76	50	7	26	87.7	65.8	75.2	+1.1
		w/	55	76	50	5	26	90.9	65.8	76.3	
E119	Exact SM	w/o	37	52	22	15	30	59.5	42.3	49.4	-3.6
		w/	31	52	19	12	33	61.3	36.5	45.8	
	PI SM	w/o	36	35	22	14	13	61.1	62.9	62.0	-3.5
		w/	30	35	19	11	16	63.3	54.3	58.5	
	Exact TM	w/o	62	96	42	20	54	67.7	43.7	53.2	-3.5
		w/	53	96	37	16	59	69.8	38.5	49.7	
	PI TM	w/o	51	58	34	17	24	66.7	58.6	62.4	-2.2
		w/	45	58	31	14	27	68.9	53.4	60.2	
Z7901	Exact SM	w/o	45	52	5	40	47	11.1	9.6	10.3	+0.5
		w/	59	52	6	53	46	10.2	11.5	10.8	
	PI SM	w/o	44	43	6	38	37	13.6	14.0	13.8	-1.8
		w/	57	43	6	51	37	10.5	14.0	12.0	
	Exact TM	w/o	167	389	71	96	318	42.5	18.3	25.5	-3.0
		w/	190	389	65	125	324	34.2	16.7	22.5	
	PI TM	w/o	138	266	78	60	188	56.5	29.3	38.6	+2.1
		w/	157	266	86	71	180	54.8	32.3	40.7	

Table 13: Plausibility results of top 5 codes. Rationales are generated by NER models. “w/o” and “w/” indicate the absence or inclusion of few-shot examples in prompts.

Dataset	MIMIC-IV ICD10 Full						MIMIC-IV ICD10 Top-50						MIMIC-III ICD9 Full						MIMIC-III ICD9 Top-50					
	FI-Mac	FI-Mic	AUC-Mac	AUC-Mic	P@8	Retention	FI-Mac	FI-Mic	AUC-Mac	AUC-Mic	P@5	Retention	FI-Mac	FI-Mic	AUC-Mac	AUC-Mic	P@8	Retention	FI-Mac	FI-Mic	AUC-Mac	AUC-Mic	P@5	Retention
Threshold	15.82	54.87	91.01	98.52	66.09	100.00	65.78	71.23	91.95	94.38	63.53	100.00	9.93	50.84	81.87	97.46	70.81	100.00	55.62	63.98	89.77	92.56	63.32	100.00
-																								
Top-P Sufficiency																								
10%	7.72	30.00	79.09	93.61	43.63	12.05	56.90	62.76	86.23	89.17	46.09	15.18	5.05	17.82	67.95	91.84	41.54	10.99	33.45	35.69	80.55	81.50	40.45	15.26
20%	9.15	35.42	83.97	96.15	48.90	21.83	58.97	64.85	88.49	91.28	47.03	24.61	6.03	22.82	71.79	93.81	49.18	20.88	37.31	40.27	83.23	85.25	42.66	24.67
30%	10.12	38.88	86.22	97.11	52.09	31.60	60.10	65.96	89.57	92.30	47.63	34.03	6.61	26.53	74.28	94.95	53.59	30.77	40.55	44.19	85.06	87.68	44.26	34.09
40%	10.83	41.33	87.76	97.61	54.35	41.37	60.87	66.70	90.16	92.92	48.07	43.45	7.02	29.41	75.92	95.66	56.65	40.66	43.01	47.22	86.31	89.15	45.41	43.51
50%	11.36	43.16	88.76	97.91	55.99	51.14	61.48	67.28	90.60	93.36	48.42	52.88	7.33	31.81	76.87	96.18	58.81	50.55	44.88	49.53	87.17	90.09	46.27	52.92
60%	11.81	44.61	89.49	98.13	57.29	60.91	61.97	67.74	90.94	93.69	48.71	62.30	7.56	33.76	78.02	96.55	60.42	60.44	46.24	51.28	87.82	90.77	46.91	62.34
70%	12.19	45.78	90.04	98.27	58.33	70.68	62.38	68.13	91.20	93.95	48.94	71.73	7.74	35.34	78.43	96.73	61.67	70.33	47.26	52.63	88.33	91.29	47.39	71.75
80%	15.14	53.93	90.47	98.38	65.24	80.46	62.73	68.45	91.46	94.17	49.14	81.15	7.88	36.65	78.76	96.85	62.68	80.22	48.03	53.68	88.71	91.65	47.78	81.17
90%	15.39	54.21	90.78	98.46	65.47	90.23	62.02	68.73	91.71	94.37	49.33	90.58	8.01	37.77	79.06	96.96	63.51	90.11	48.62	54.51	89.23	92.11	48.11	90.38
Top-P Completeness																								
10%	12.62	46.54	89.17	97.92	57.84	90.23	13.72	15.39	71.68	71.27	22.78	90.38	2.80	13.54	75.15	95.37	35.25	90.11	8.62	9.66	75.71	74.72	25.31	90.38
20%	11.97	43.43	87.35	97.17	54.37	80.46	12.73	14.58	67.88	67.80	21.55	81.15	2.59	12.32	72.10	93.60	31.17	80.22	6.90	7.75	66.85	65.97	26.49	81.17
30%	11.33	40.59	85.54	96.34	51.17	70.68	11.97	14.03	65.01	65.33	20.63	71.73	2.45	11.31	69.62	92.06	28.28	70.33	6.20	6.98	60.43	61.35	24.80	71.75
40%	10.73	37.82	84.00	95.44	48.03	60.91	11.29	13.55	62.51	63.21	19.82	62.30	2.36	10.56	67.50	90.71	26.04	60.44	5.84	6.59	56.08	58.58	23.64	62.34
50%	10.11	34.98	82.40	94.31	44.93	51.14	10.74	13.18	60.01	61.34	19.10	52.88	2.29	9.84	65.22	89.41	24.06	50.55	5.77	6.49	53.10	56.58	22.77	52.92
60%	9.46	31.89	80.53	92.84	41.79	41.37	10.29	12.86	57.61	59.61	18.43	43.45	2.20	9.07	63.41	88.11	22.34	40.66	5.77	6.50	50.71	54.94	22.07	43.51
70%	8.77	28.38	78.43	90.86	38.64	31.60	9.87	12.55	55.22	58.08	17.85	34.03	2.13	8.34	61.66	86.76	20.79	30.77	5.80	6.54	48.70	53.44	21.47	34.09
80%	4.16	7.99	75.30	87.81	12.98	21.83	9.52	12.28	53.15	56.62	17.31	24.61	2.00	7.30	59.62	84.65	19.27	20.88	5.90	6.62	47.25	51.91	20.91	24.67
90%	3.17	4.81	70.84	82.12	9.55	12.05	9.23	12.09	51.01	55.13	16.79	15.18	1.76	5.64	56.38	80.38	17.70	10.99	6.03	6.79	46.07	50.32	20.31	15.26
Top-N Sufficiency																								
20%	9.13	34.64	81.37	94.70	48.39	16.61	56.68	64.53	87.02	89.94	46.77	19.11	5.78	22.00	70.01	92.67	45.67	14.24	35.27	37.86	81.21	82.40	41.27	18.07
40%	10.49	39.54	85.53	96.75	52.93	30.71	60.24	66.10	88.97	91.81	47.62	32.37	6.70	27.69	73.45	94.47	52.63	27.31	39.15	42.49	83.81	85.96	43.44	30.24
60%	11.40	42.44	87.53	97.52	55.60	44.48	61.19	67.01	89.91	92.70	48.17	45.39	7.26	31.74	75.62	95.55	56.68	40.06	42.15	46.12	85.34	88.03	44.92	42.10
80%	12.03	44.48	88.84	97.91	57.44	57.43	61.87	67.65	90.47	93.26	48.57	57.80	7.61	34.56	77.10	96.14	59.25	52.18	44.37	48.85	86.42	89.31	45.98	53.37
100%	12.51	45.99	89.60	98.14	58.79	68.87	62.36	68.13	90.89	93.67	48.88	68.93	7.86	36.70	77.82	96.54	61.09	63.17	46.04	50.93	87.28	90.25	46.74	63.74
120%	12.90	47.16	90.12	98.28	59.82	78.15	62.76	68.51	91.23	93.97	49.13	78.06	8.06	38.36	78.55	96.79	62.45	72.61	47.28	52.51	87.87	90.88	47.29	72.84
140%	13.22	48.08	90.47	98.37	60.60	85.12	63.10	68.83	91.46	94.17	49.33	84.98	8.22	39.67	79.14	96.95	63.49	80.17	48.26	53.77	88.36	91.37	47.74	80.22
160%	13.48	48.82	90.66	98.42	61.24	90.08	63.38	69.09	91.63	94.31	49.53	89.96	8.35	40.72	79.77	97.08	64.32	85.94	49.01	54.77	88.80	91.74	48.10	85.89
180%	13.70	49.43	90.80	98.46	61.75	93.53	63.61	69.30	91.73	94.40	49.68	93.44	8.45	41.60	80.12	97.18	64.98	90.27	49.62	55.60	89.13	92.04	48.40	90.12
200%	13.88	49.93	90.91	98.48	62.16	95.83	63.81	69.48	91.83	94.47	49.81	95.78	8.54	42.34	80.71	97.27	65.53	93.42	50.13	56.29	89.31	92.22	48.66	93.19
Top-N Completeness																								
20%	11.34	43.65	88.26	97.59	54.84	85.74	13.28	15.04	70.03	69.81	21.82	86.64	2.61	12.73	73.94	94.75	32.95	86.85	8.94	9.69	75.65	72.90	28.46	87.77
40%	10.36	38.18	85.78	96.38	50.36	71.64	12.20	14.23	65.25	65.56	20.45	73.38	2.23	9.66	69.99	92.10	28.98	73.79	7.12	7.84	64.24	64.55	25.90	75.60
60%	9.01	30.66	83.31	94.65	46.05	57.88	11.31	13.56	61.39	62.41	19.33	60.37	1.72	5.81	63.97	88.96	26.00	61.04	6.47	7.24	57.57	59.46	24.28	63.74
80%	7.68	22.08	80.22	91.89	44.97	44.93	10.65	13.11	57.83	59.62	18.42	47.97	1.33	3.46	62.26	85.06	23.73	48.93	6.44	7.24	53.60	56.45	23.17	52.48
100%	6.57	15.14	75.95	87.71	38.13	33.49	10.23	12.83	54.67	57.22	17.64	36.84	1.07	2.13	58.04	78.98	21.75	37.94	6.67	7.49	50.47	53.68	22.27	42.11
120%	5.64	10.44	71.41	82.43	34.66	24.20	10.05	12.74	52.30	55.32	16.98	27.72	0.90	1.48	54.52	71.60	19.98	28.51	7.13	7.97	48.31	51.47	21.46	33.02
140%	4.86	7.46	66.94	76.88	31.51	17.24	10.09	12.79	50.84	54.03	16.41	20.82	0.81	1.15	51.21	63.38	18.37	20.96	7.90	8.81	47.03	49.90	20.72	25.65
160%	4.25	5.59	63.48	71.81	28.69	12.27	10.28	12.99	50.20	53.37	15.95	15.84	0.76	0.99	49.37	56.65	16.90	15.20	8.81	9.77	46.88	49.36	20.05	19.99
180%	3.77	4.37	60.59	67.37	26.21	8.82	10.57	13.26	50.11	53.05	15.56	12.37	0.74	0.91	48.38	50.96	15.60	10.87	9.69	10.70	47.67	49.45	19.42	15.77
200%	3.38	3.54	58.38	63.85	24.04	6.52	10.86	13.54	50.05	52.83	15.24	10.04	0.74	0.86	47.53	45.64	14.42	7.73	10.46	11.51	48.06	49.45	18.89	12.70

Table 14: Faithfulness across Top-P and Top-N thresholds for CAML.



Dataset	MIMIC-IV ICD10 Full					MIMIC-IV ICD10 Top-50					MIMIC-III ICD9 Full					MIMIC-III ICD9 Top-50								
	FI-Mac	FI-Mic	AUC-Mac	AUC-Mic	P@8	Retention	FI-Mac	FI-Mic	AUC-Mac	AUC-Mic	P@5	Retention	FI-Mac	FI-Mic	AUC-Mac	AUC-Mic	P@8	Retention	FI-Mac	FI-Mic	AUC-Mac	AUC-Mic	P@5	Retention
Threshold	20.88	57.86	95.25	99.02	68.98	100.00	67.50	72.93	92.76	95.22	64.68	100.00	16.89	56.53	89.94	98.59	74.35	100.00	59.51	67.58	90.27	93.06	64.23	100.00
Top-P Sufficiency																								
10%	11.45	44.53	86.80	95.28	58.37	11.27	54.99	62.98	85.39	88.65	46.10	15.52	11.37	46.26	85.83	97.08	64.55	10.21	52.02	58.64	83.99	87.42	46.96	13.64
20%	13.25	47.59	91.60	97.41	60.88	21.13	56.29	64.03	87.06	90.26	46.77	24.90	12.50	48.08	88.33	98.03	66.49	20.19	52.83	60.24	86.34	89.58	48.04	23.24
30%	14.50	49.56	93.32	98.26	62.45	30.99	57.52	65.06	88.26	91.31	47.26	34.29	13.32	49.43	89.27	98.33	67.78	30.17	53.69	61.36	87.34	90.41	48.71	32.83
40%	15.41	50.97	94.22	98.67	63.57	40.85	58.62	65.98	89.18	92.10	47.68	43.68	13.93	50.48	89.71	98.46	68.73	40.14	54.43	62.26	87.90	90.93	49.18	42.43
50%	16.13	52.03	94.77	98.86	64.41	50.71	59.59	66.80	89.89	92.75	48.05	53.07	14.38	51.28	89.82	98.51	69.45	50.12	55.01	62.94	88.42	91.41	49.55	52.02
60%	19.97	56.98	95.00	98.94	68.21	60.56	64.36	70.85	90.47	93.27	50.09	62.45	14.76	51.96	89.88	98.55	70.07	60.09	55.61	63.56	88.72	91.67	49.83	61.62
70%	20.26	57.19	95.14	98.99	68.42	70.42	64.75	71.14	90.98	93.70	50.32	71.84	15.06	52.51	89.99	98.58	70.59	70.07	56.09	64.05	88.95	91.90	50.03	71.21
80%	20.42	57.35	95.21	99.01	68.56	80.28	65.12	71.40	91.42	94.07	50.50	81.23	15.31	52.98	89.97	98.59	71.02	80.05	56.48	64.46	89.16	92.10	50.20	80.81
90%	20.54	57.47	95.24	99.02	68.66	90.14	65.44	71.62	91.83	94.42	50.68	90.61	15.52	53.36	89.94	98.59	71.38	90.02	56.78	64.77	89.45	92.38	50.36	90.40
Top-P Comprehensiveness																								
10%	5.90	14.43	85.66	91.47	21.73	90.14	15.77	20.19	69.27	70.31	25.00	90.61	2.39	7.33	80.53	92.92	23.70	90.02	7.68	7.96	62.84	63.57	19.57	90.47
20%	4.34	10.77	77.83	83.95	17.50	80.28	15.22	19.52	66.17	68.42	24.11	81.23	1.88	5.67	73.83	87.92	19.30	80.05	8.41	8.97	59.67	61.86	18.67	80.81
30%	3.27	7.78	72.15	77.07	14.34	70.42	14.71	18.97	65.25	67.92	23.54	71.84	1.51	4.65	68.47	83.20	16.41	70.07	8.89	9.68	56.78	59.30	17.97	71.21
40%	2.56	5.65	67.33	71.21	11.99	60.56	14.24	18.45	63.84	66.99	23.01	62.45	1.25	3.89	64.77	78.88	14.28	60.09	9.18	10.32	54.80	57.49	17.38	61.62
50%	2.06	4.21	63.59	66.04	10.22	50.70	13.77	17.94	62.40	65.94	22.50	53.07	1.08	3.35	60.95	75.10	12.68	50.12	9.54	11.06	53.46	56.25	16.95	52.02
60%	1.71	3.23	60.37	61.71	8.88	40.85	10.87	15.05	61.12	64.87	19.57	43.68	0.95	2.91	58.32	72.20	11.46	40.14	9.97	11.90	52.96	55.64	16.67	42.43
70%	1.45	2.58	57.71	58.40	7.85	30.99	10.38	14.56	59.83	63.70	19.11	34.29	0.84	2.57	55.99	69.88	10.56	30.17	10.42	12.78	52.18	55.13	16.42	32.83
80%	1.25	2.12	55.03	55.81	7.05	21.13	9.92	14.14	58.43	62.36	18.59	24.90	0.76	2.32	54.76	68.51	9.91	20.19	11.03	13.84	52.02	55.36	16.28	23.24
90%	1.10	1.80	52.68	53.55	6.43	11.27	9.44	13.72	56.58	60.63	18.11	15.52	0.69	2.12	53.34	68.02	9.54	10.21	11.82	14.94	51.16	55.25	16.11	13.64
Top-N Sufficiency																								
20%	12.84	46.95	88.98	96.19	60.47	15.89	55.77	63.64	86.06	89.36	46.58	19.41	11.75	46.78	86.56	97.33	65.59	13.54	52.11	59.00	84.54	87.84	46.93	16.57
40%	14.54	49.51	92.65	97.88	62.66	30.15	57.42	65.03	87.69	90.96	47.31	32.54	13.01	48.65	88.77	98.15	67.36	26.75	53.35	60.86	86.52	89.81	48.23	28.97
60%	15.64	51.16	93.94	98.51	64.01	44.07	58.77	66.18	88.87	92.00	47.87	45.44	13.77	49.93	89.43	98.38	68.50	39.64	54.18	61.93	87.33	90.57	48.93	41.06
80%	16.44	52.31	94.58	98.78	64.92	57.14	59.90	67.12	89.85	92.84	48.35	57.75	14.30	50.89	89.81	98.49	69.41	51.86	54.89	62.76	87.86	91.08	49.39	52.55
100%	17.05	53.17	94.91	98.91	65.59	68.68	60.85	67.89	90.64	93.48	48.75	68.84	14.65	51.64	89.88	98.54	70.12	62.96	55.46	63.40	88.28	91.46	49.74	63.13
120%	17.52	53.83	95.08	98.96	66.08	78.02	61.65	68.51	91.22	93.98	49.11	77.97	14.97	52.25	89.98	98.57	70.66	72.47	55.94	63.91	88.74	91.79	50.02	72.57
140%	17.90	54.35	95.16	98.99	66.46	85.01	62.33	69.03	91.67	94.35	49.41	84.89	15.21	52.73	89.98	98.58	71.09	80.07	56.35	64.32	89.05	92.06	50.25	79.90
160%	18.21	54.75	95.21	99.01	66.76	90.01	66.76	90.01	92.01	94.62	49.67	89.89	15.41	53.13	89.97	98.59	71.46	85.87	56.68	64.66	89.36	92.33	50.44	85.69
180%	18.47	55.08	95.23	99.02	67.00	93.48	63.39	69.81	92.27	94.82	49.88	93.38	15.57	53.47	89.95	98.59	71.76	90.23	56.96	64.95	89.60	92.52	50.59	89.99
200%	18.68	55.36	95.24	99.02	67.20	95.79	63.80	70.11	92.44	94.96	50.07	95.73	15.70	53.76	89.98	98.59	72.01	93.39	57.20	65.19	89.83	92.69	50.73	93.11
Top-N Comprehensiveness																								
20%	4.72	11.97	81.88	88.43	18.72	85.59	15.43	19.69	67.47	69.24	24.55	86.79	2.18	6.93	78.28	91.80	21.51	86.70	7.80	8.17	59.45	61.31	18.78	87.54
40%	3.18	7.68	72.90	78.43	14.45	71.33	14.84	18.98	64.41	67.36	23.64	73.66	1.72	5.39	70.28	85.41	17.43	73.48	8.52	9.12	55.56	58.15	17.72	75.14
60%	2.23	5.03	66.68	70.84	11.59	57.42	14.27	18.34	62.68	66.01	22.86	60.75	1.38	4.31	65.42	80.03	14.75	60.60	8.74	9.71	53.09	56.02	16.94	63.05
80%	1.68	3.50	61.99	64.58	9.61	44.34	13.68	17.67	60.24	63.85	22.11	48.44	1.13	3.57	61.46	75.33	12.79	48.38	9.05	10.45	51.28	54.31	16.46	51.56
100%	1.32	2.56	58.09	59.34	8.21	32.80	13.20	17.15	57.50	61.26	21.41	37.36	0.94	2.97	57.55	70.94	11.42	37.29	9.65	11.40	50.56	53.52	16.23	40.99
120%	1.08	1.96	55.20	55.40	7.16	23.46	12.88	16.78	54.74	58.60	20.74	28.23	0.79	2.49	54.98	67.07	10.43	27.79	10.42	12.42	49.43	52.42	16.03	31.74
140%	0.92	1.58	53.29	52.91	6.37	16.47	12.73	16.62	52.94	56.87	20.15	26.30	0.69	2.14	52.21	64.16	9.76	20.20	11.30	13.45	48.94	51.89	15.85	24.21
160%	0.81	1.34	51.77	51.57	5.74	11.47	12.77	16.64	52.16	56.09	19.64	16.30	0.62	1.87	50.90	61.69	9.25	14.41	12.20	14.42	48.94	51.60	15.71	18.42
180%	0.72	1.16	51.17	50.82	5.24	8.01	12.90	16.77	51.97	55.86	19.20	12.81	0.56	1.67	50.13	60.20	8.88	10.06	13.03	15.25	49.16	51.61	15.56	14.12
200%	0.66	1.04	50.79	50.41	4.84	5.69	13.09	16.98	52.10	56.01	18.82	10.46	0.52	1.52	49.07	58.83	8.58	6.90	13.76	15.96	49.13	51.34	15.40	11.00

Table 15: Faithfulness across Top-P and Top-N thresholds for LAAT.

Dataset	MIMIC-IV ICD10 Full					MIMIC-IV ICD10 Top-50					MIMIC-III ICD9 Full					MIMIC-III ICD9 Top-50								
	FI-Mac	FI-Mic	AUC-Mac	AUC-Mic	P@8	Retention	FI-Mac	FI-Mic	AUC-Mac	AUC-Mic	P@5	Retention	FI-Mac	FI-Mic	AUC-Mac	AUC-Mic	P@8	Retention	FI-Mac	FI-Mic	AUC-Mac	AUC-Mic	P@5	Retention
Threshold	19.70	58.32	96.54	99.23	69.79	100.00	68.20	73.42	93.30	95.50	65.35	100.00	16.20	56.33	91.39	98.75	73.10	100.00	65.70	71.18	91.96	94.26	66.65	100.00
Top-P Sufficiency																								
10%	6.44	47.05	83.04	95.21	62.86	11.35	63.49	70.12	89.09	91.99	49.64	14.97	12.34	46.90	79.79	95.24	66.51	10.37	58.83	66.03	86.02	88.14	49.45	12.13
20%	7.63	48.99	90.07	96.94	63.98	21.20	64.37	70.62	91.10	93.70	50.18	24.42	13.74	47.72	84.76	96.75	67.03	20.33	61.03	67.52	88.34	90.80	50.66	21.89
30%	8.44	50.22	92.80	97.79	64.69	31.05	65.07	71.06	92.16	94.56	50.60	33.87	14.47	48.70	87.65	97.73	67.62	30.29	61.95	68.18	89.24	91.75	51.23	31.66
40%	8.99	51.10	94.25	98.27	65.24	40.90	65.56	71.40	92.67	94.97	50.89	43.31	15.00	49.58	89.16	98.19	68.11	40.25	62.59	68.62	90.13	92.55	51.66	41.42
50%	10.98	54.48	95.11	98.55	67.60	50.75	67.42	72.76	92.91	95.19	51.99	52.76	15.36	50.34	89.79	98.42	68.56	50.21	63.05	68.92	90.62	93.16	52.01	51.19
60%	11.40	54.85	95.70	98.76	67.90	60.60	67.54	72.87	93.09	95.33	52.08	62.21	15.54	51.02	90.56	98.59	69.04	60.17	63.37	69.17	90.95	93.51	52.27	60.95
70%	11.90	55.27	96.06	98.92	68.19	70.45	67.66	72.98	93.20	95.42	52.13	71.66	15.66	51.60	90.87	98.67	69.48	70.12	63.62	69.36	91.33	93.84	52.48	70.71
80%	12.62	55.70	96.31	99.05	68.45	80.30	67.76	73.06	93.24	95.46	52.18	81.10	15.76	52.07	91.19	98.72	69.85	80.08	63.85	69.56	91.54	93.95	52.65	80.48
90%	13.60	56.14	96.45	99.16	68.68	90.15	67.84	73.13	93.27	95.48	52.22	90.55	15.82	52.48	91.27	98.73	70.19	90.04	64.01	69.69	91.85	94.15	52.79	90.24
Top-P Comprehensiveness																								
10%	7.30	24.37	91.34	96.93	37.00	90.15	15.25	16.14	73.90	73.50	24.12	90.55	10.40	32.43	87.87	97.42	46.89	90.04	38.46	41.69	83.08	84.77	40.01	90.24
20%	5.36	18.05	83.41	93.87	30.82	80.30	12.16	12.73	66.44	66.82	21.74	81.10	8.47	25.96	80.34	95.11	39.04	80.08	32.28	34.74	78.77	79.37	36.65	80.48
30%	4.26	14.22	76.66	91.42	27.09	70.45	10.16	10.54	61.77	63.63	20.44	71.66	7.01	21.37	73.10	93.16	33.48	70.12	27.32	29.38	75.10	74.74	33.91	70.71
40%	3.53	11.69	70.78	89.94	24.74	60.60	8.70	8.96	58.63	61.90	19.64	62.21	5.99	18.10	66.40	91.71	29.53	60.17	23.54	25.31	72.09	71.52	31.89	60.95
50%	3.02	9.90	65.45	89.12	23.24	50.75	7.58	7.78	57.07	61.26	19.15	52.76	5.23	15.69	62.50	89.90	26.54	50.21	20.60	22.17	69.27	68.95	30.31	51.19
60%	2.64	8.56	60.53	88.62	22.35	40.90	6.71	6.86	56.82	61.15	18.82	43.31	4.64	13.77	59.32	89.89	24.49	40.25	18.33	19.74	67.22	67.14	29.10	41.42
70%	2.35	7.52	56.61	88.29	21.83	31.05	6.01	6.13	57.30	61.09	18.55	33.87	4.18	12.25	58.10	89.60	23.03	30.29	16.48	17.75	65.25	65.53	28.12	31.66
80%	2.12	6.69	53.49	88.08	21.56	21.20	5.44	5.53	57.41	60.70	18.29	24.42	3.79	11.01	55.17	87.56	21.89	20.33	14.92	16.05	63.51	64.04	27.23	21.89
90%	1.94	6.02	51.72	87.96	21.39	11.35	4.97	5.04	56.85	60.06	18.02	14.97	3.47	9.99	55.20	86.69	20.98	10.37	13.60	14.62	60.28	62.37	26.39	12.13
Top-N Sufficiency																								
20%	6.68	46.56	82.04	94.81	63.10	13.21	63.51	70.14	88.90	91.86	49.70	16.38	12.20	47.59	80.72	95.53	66.95	11.42	57.96	65.62	84.96	87.67	49.35	12.92
40%	7.93	48.63	87.60	96.50	64.23	24.86	64.36	70.64	91.01	93.62	50.22	27.21	13.81	48.75	83.80	97.19	67.70	22.39	60.40	67.27	88.02	90.56	50.46	23.43
60%	8.69	49.90	90.89	97.38	64.97	36.39	64.99	71.05	92.05	94.46	50.61	37.96	14.54	49.46	87.83	97.70	68.10	33.25	61.59	68.05	89.17	91.68	51.15	33.89
80%	9.39	50.82	92.64	97.92	65.54	47.62	65.45	71.35	92.56	94.88	50.89	48.52	15.00	50.17	88.95	98.15	68.54	43.83	62.20	68.43	89.49	92.17	51.53	44.03
100%	10.07	51.57	93.58	98.26	66.03	58.23	65.82	71.61	92.87	95.14	51.11	58.61	15.34	50.78	89.56	98.34	68.92	53.95	62.67	68.76	90.26	92.90	51.87	53.78
120%	10.77	52.19	94.08	98.46	66.43	67.72	66.12	71.83	93.04	95.28	51.27	67.79	15.59	51.35	90.18	98.52	69.32	63.27	63.00	68.97	90.60	93.26	52.13	62.87
140%	11.48	52.73	94.46	98.63	66.77	75.87	66.35	72.00	93.12	95.36	51.40	75.77	15.76	51.83	90.58	98.60	69.69	71.39	63.30	69.18	90.85	93.47	52.36	71.06
160%	12.17	53.20	94.77	98.75	67.06	82.28	66.55	72.14	93.18	95.41	51.51	82.10	15.88	52.24	90.84	98.66	70.01	78.51	63.53	69.36	91.12	93.71	52.53	78.05
180%	12.81	53.62	95.07	98.86	67.30	87.34	66.72	72.27	93.24	95.45	51.60	87.17	15.97	52.61	91.05	98.70	70.29	84.22	63.73	69.53	91.29	93.85	52.69	83.80
200%	13.40	54.00	95.35	98.94	67.52	91.04	66.85	72.37	93.27	95.48	51.67	90.90	16.03	52.92	91.17	98.72	70.54	88.72	63.91	69.68	91.49	93.95	52.82	88.40
Top-N Comprehensiveness																								
20%	7.62	25.40	86.84	96.09	36.33	88.29	15.97	16.63	73.93	73.84	24.28	89.14	10.08	32.48	85.62	96.80	45.67	88.99	40.28	43.28	83.21	84.77	40.15	89.45
40%	5.78	19.40	77.83	93.40	30.79	76.64	12.82	13.18	66.56	67.30	22.02	78.31	8.43	26.82	77.48	94.37	38.55	78.02	33.70	36.13	79.05	79.66	36.90	78.94
60%	4.63	15.58	71.39	91.60	27.45	65.12	10.76	10.96	61.95	64.05	20.75	67.56	7.14	22.64	71.13	92.77	33.69	67.16	28.81	30.85	75.42	75.48	34.27	68.48
80%	3.86	12.96	65.87	90.45	25.38	53.89	9.29	9.38	58.48	62.18	19.93	57.01	6.19	19.50	66.61	91.73	30.19	56.39	25.24	26.91	72.29	72.17	32.33	58.34
100%	3.31	11.06	62.46	89.71	24.04	43.29	8.16	8.20	56.39	61.22	19.37	46.91	5.44	17.09	63.23	91.21	27.64	46.48	22.32	23.82	69.51	69.70	30.77	48.39
120%	2.90	9.63	59.59	89.23	23.18	33.79	7.29	7.30	55.73	60.91	18.97	37.74	4.88	15.17	61.40	90.65	25.64	37.15	20.03	21.40	67.39	67.87	29.59	39.30
140%	2.59	8.51	57.53	88.87	22.59	25.66	6.57	6.56	55.54	60.65	18.64	29.78	4.40	13.61	59.70	90.39	24.08	28.85	18.15	17.40	64.78	66.07	28.57	31.31
160%	2.34	7.61	56.37	88.60	22.19	19.26	5.98	5.96	56.16	60.63	18.37	23.44	4.01	12.32	58.11	89.53	22.84	21.93	16.54	17.70	62.89	64.86	27.67	24.33
180%	2.13	6.88	55.84	88.40	21.92	14.20	5.49	5.46	56.70	60.48	18.14	18.39	3.68	11.23	56.84	89.46	21.86	16.23	15.20	16.28	61.31	63.78	26.92	18.37
200%	1.97	6.27	54.88	88.26	21.72	10.5	5.08	5.04	57.10	60.41	17.93	14.66	3.40	10.30	56.25	89.02	21.01	11.73	14.05	15.04	59.85	63.07	26.27	13.97

Table 16: Faithfulness across Top-P and Top-N thresholds for PLM-ICD.



Table 18: Plausibility results of LAAT across all thresholds.

(a) Results using the Top-p selection strategy.											(b) Results using the Top-N selection strategy.										
Metric	Threshold	#Ptd	#Act	TP	FP	FN	Pt	Rc	F1		Metric	Threshold	#Ptd	#Act	TP	FP	FN	Pt	Rc	F1	
Exact SM	0.1	91482	2269	330	91152	1939	0.4%	14.5%	0.7%		Exact SM	200	109729	2269	291	109438	1978	0.3%	12.8%	0.5%	
	0.2	152195	2269	183	152012	2086	0.1%	8.1%	0.2%			400	171537	2269	124	171413	2145	0.1%	5.5%	0.1%	
	0.3	190875	2269	107	190768	2162	0.1%	4.7%	0.1%			600	200746	2269	75	200671	2194	0.0%	3.3%	0.1%	
	0.4	211973	2269	62	211911	2207	0.0%	2.7%	0.1%			800	202268	2269	38	202230	2231	0.0%	1.7%	0.0%	
	0.5	217293	2269	40	217253	2229	0.0%	1.8%	0.0%			1000	178051	2269	19	178032	2250	0.0%	0.8%	0.0%	
	0.6	207522	2269	29	207493	2240	0.0%	1.3%	0.0%			1200	138551	2269	12	138539	2257	0.0%	0.5%	0.0%	
	0.7	182928	2269	15	182913	2254	0.0%	0.7%	0.0%			1400	97825	2269	4	97821	2265	0.0%	0.2%	0.0%	
	0.8	143185	2269	3	143182	2266	0.0%	0.1%	0.0%			1600	64925	2269	3	64922	2266	0.0%	0.1%	0.0%	
	0.9	87373	2269	1	87372	2268	0.0%	0.0%	0.0%			1800	37745	2269	2	37743	2267	0.0%	0.1%	0.0%	
PI SM	0.1	82542	2021	342	82200	1679	0.4%	16.9%	0.8%		PI SM	2000	21659	2269	3	21656	2266	0.0%	0.1%	0.0%	
	0.2	138074	2021	223	137851	1798	0.2%	11.0%	0.3%			200	99384	2021	305	99079	1716	0.3%	15.1%	0.6%	
	0.3	174708	2021	145	174563	1876	0.1%	7.2%	0.2%			400	156766	2021	165	156601	1856	0.1%	8.2%	0.2%	
	0.4	196066	2021	102	195964	1919	0.1%	5.0%	0.1%			600	185712	2021	120	185592	1901	0.1%	5.9%	0.1%	
	0.5	203071	2021	74	202997	1947	0.0%	3.7%	0.1%			800	189014	2021	72	188942	1949	0.0%	3.6%	0.1%	
	0.6	195899	2021	55	195844	1966	0.0%	2.7%	0.1%			1000	167363	2021	51	167312	1970	0.0%	2.5%	0.1%	
	0.7	174663	2021	41	174622	1980	0.0%	2.0%	0.0%			1200	130794	2021	38	130756	1983	0.0%	1.9%	0.1%	
	0.8	138486	2021	24	138462	1997	0.0%	1.2%	0.0%			1400	93001	2021	14	92987	2007	0.0%	0.7%	0.0%	
	0.9	85688	2021	11	85677	2010	0.0%	0.5%	0.0%			1600	61976	2021	7	61969	2014	0.0%	0.3%	0.0%	
Exact TM	0.1	160732	11428	4266	156466	7162	2.7%	37.3%	5.0%		Exact TM	1800	35988	2021	5	35983	2016	0.0%	0.2%	0.0%	
	0.2	316121	11428	4840	311281	6588	1.5%	42.4%	3.0%			2000	20502	2021	5	20497	2016	0.0%	0.2%	0.0%	
	0.3	467215	11428	5258	461957	6170	1.1%	46.0%	2.2%			200	206362	11428	4482	201880	6946	2.2%	39.2%	4.1%	
	0.4	615384	11428	5468	609916	5960	0.9%	47.8%	1.7%			400	404155	11428	5093	399062	6335	1.3%	44.6%	2.5%	
	0.5	759735	11428	5539	754196	5889	0.7%	48.5%	1.4%			600	596166	11428	5414	590752	6014	0.9%	47.4%	1.8%	
	0.6	901596	11428	5961	895635	5467	0.7%	52.2%	1.3%			800	782134	11428	5637	776497	5791	0.7%	49.3%	1.4%	
	0.7	1040440	11428	6142	1034298	5286	0.6%	53.7%	1.2%			1000	959318	11428	5701	953617	5727	0.6%	49.9%	1.2%	
	0.8	1175547	11428	6022	1169525	5406	0.5%	52.7%	1.0%			1200	1104095	11428	5811	1098284	5617	0.5%	50.8%	1.0%	
	0.9	1303770	11428	5812	1297958	5616	0.4%	50.9%	0.9%			1400	1217029	11428	5727	1211302	5701	0.5%	50.1%	0.9%	
PI TM	0.1	121292	9367	4720	116572	4647	3.9%	50.4%	7.2%		PI TM	1600	1294041	11428	5943	1288098	5485	0.5%	52.0%	0.9%	
	0.2	212105	9367	5732	206373	3635	2.7%	61.2%	5.2%			1800	1343294	11428	5736	1337558	5692	0.4%	50.2%	0.8%	
	0.3	284284	9367	6234	278050	3133	2.2%	66.6%	4.2%			2000	1368335	11428	5417	1362918	6011	0.4%	47.4%	0.8%	
	0.4	344568	9367	6705	337863	2662	1.9%	71.6%	3.8%			200	150423	9367	5104	145319	4263	3.4%	54.5%	6.4%	
	0.5	394117	9367	6979	387138	2388	1.8%	74.5%	3.5%			400	225097	9367	6039	249058	3328	2.4%	64.5%	4.6%	
	0.6	436327	9367	7249	429078	2118	1.7%	77.4%	3.3%			600	336224	9367	6659	329565	2708	2.0%	71.1%	3.9%	
	0.7	470428	9367	7420	463008	1947	1.6%	79.2%	3.1%			800	400263	9367	7100	393163	2267	1.8%	75.8%	3.5%	
	0.8	498098	9367	7545	490553	1822	1.5%	80.5%	3.0%			1000	452497	9367	7337	445160	2030	1.6%	78.3%	3.2%	
	0.9	523255	9367	7637	515618	1730	1.5%	81.5%	2.9%			1200	490632	9367	7612	483020	1755	1.6%	81.3%	3.0%	

Table 19: Plausibility results of PLM-ICD across all thresholds.

(a) Results using the Top-p selection strategy.

Metric	Threshold	#Ptd	#Act	TP	FP	FN	Pt	Rc	F1
Exact SM	10%	65639	2269	172	65467	2097	0.3%	7.6%	0.5%
	20%	99489	2269	112	99377	2157	0.1%	4.9%	0.2%
	30%	117733	2269	68	117665	2201	0.1%	3.0%	0.1%
	40%	123897	2269	48	123849	2221	0.0%	2.1%	0.1%
	50%	123055	2269	38	123017	2231	0.0%	1.7%	0.1%
	60%	112511	2269	23	112488	2246	0.0%	1.0%	0.0%
	70%	96512	2269	14	96498	2255	0.0%	0.6%	0.0%
	80%	72706	2269	8	72698	2261	0.0%	0.4%	0.0%
	90%	44799	2269	2	44797	2267	0.0%	0.1%	0.0%
PI SM	10%	60851	2041	228	60623	1813	0.4%	11.2%	0.7%
	20%	91601	2041	173	91428	1868	0.2%	8.5%	0.4%
	30%	108523	2041	125	108398	1916	0.1%	6.1%	0.2%
	40%	114615	2041	109	114506	1932	0.1%	5.3%	0.2%
	50%	113966	2041	89	113877	1952	0.1%	4.4%	0.2%
	60%	104917	2041	63	104854	1978	0.1%	3.1%	0.1%
	70%	90569	2041	46	90523	1995	0.1%	2.3%	0.1%
	80%	68893	2041	29	68864	2012	0.0%	1.4%	0.1%
	90%	42952	2041	13	42939	2028	0.0%	0.6%	0.1%
Exact TM	10%	173633	12517	3975	169658	8542	2.3%	31.8%	4.3%
	20%	332771	12517	4194	328577	8323	1.3%	33.5%	2.4%
	30%	486349	12517	4251	482098	8266	0.9%	34.0%	1.7%
	40%	641050	12517	4256	636794	8261	0.7%	34.0%	1.3%
	50%	795367	12517	4168	791199	8349	0.5%	33.3%	1.0%
	60%	949630	12517	4015	945615	8502	0.4%	32.1%	0.8%
	70%	1100798	12517	4189	1096609	8328	0.4%	33.5%	0.8%
	80%	1246480	12517	4106	1242374	8411	0.3%	32.8%	0.7%
	90%	1381492	12517	4208	1377284	8309	0.3%	33.6%	0.6%
PI TM	10%	120777	10269	5794	114983	4475	4.8%	56.4%	8.8%
	20%	203259	10269	6548	196711	3721	3.2%	63.8%	6.1%
	30%	270926	10269	7060	263866	3209	2.6%	68.8%	5.0%
	40%	332829	10269	7461	325368	2808	2.2%	72.7%	4.3%
	50%	388647	10269	7665	380982	2604	2.0%	74.6%	3.8%
	60%	439645	10269	7835	431810	2434	1.8%	76.3%	3.5%
	70%	485691	10269	8082	477609	2187	1.7%	78.7%	3.3%
	80%	526864	10269	8145	518719	2124	1.5%	79.3%	3.0%
	90%	560856	10269	8233	552623	2036	1.5%	80.2%	2.9%

(b) Results using the Top-N selection strategy.

Metric	Threshold	#Ptd	#Act	TP	FP	FN	Pt	Rc	F1
Exact SM	200	67058	2269	170	66888	2099	0.3%	7.5%	0.5%
	400	99646	2269	98	99548	2171	0.1%	4.3%	0.2%
	600	115216	2269	68	115148	2201	0.1%	3.0%	0.1%
	800	118029	2269	45	117984	2224	0.0%	2.0%	0.1%
	1000	112128	2269	31	112097	2238	0.0%	1.4%	0.1%
	1200	99278	2269	18	99260	2251	0.0%	0.8%	0.0%
	1400	81722	2269	13	81709	2256	0.0%	0.6%	0.0%
	1600	64482	2269	5	64477	2264	0.0%	0.2%	0.0%
	1800	43416	2269	4	43412	2265	0.0%	0.2%	0.0%
PI SM	2000	30369	2269	1	30368	2268	0.0%	0.0%	0.0%
	200	62197	2041	225	61972	1816	0.4%	11.0%	0.7%
	400	92102	2041	161	91941	1880	0.2%	7.9%	0.3%
	600	106563	2041	125	106438	1916	0.1%	6.1%	0.2%
	800	109437	2041	93	109344	1948	0.1%	4.6%	0.2%
	1000	104052	2041	79	103973	1962	0.1%	3.9%	0.1%
	1200	92471	2041	55	92416	1986	0.1%	2.7%	0.1%
	1400	76305	2041	40	76265	2001	0.1%	2.0%	0.1%
	1600	60330	2041	25	60305	2016	0.0%	1.2%	0.1%
Exact TM	1800	40620	2041	22	40598	2019	0.1%	1.1%	0.1%
	2000	28513	2041	14	28499	2027	0.0%	0.7%	0.1%
	200	182545	12517	3972	178573	8545	2.2%	31.7%	4.1%
	400	348662	12517	4175	344487	8342	1.2%	33.4%	2.3%
	600	509830	12517	4253	505577	8264	0.8%	34.0%	1.6%
	800	672002	12517	4313	667689	8204	0.6%	34.5%	1.3%
	1000	834402	12517	4207	830195	8310	0.5%	33.6%	1.0%
	1200	989036	12517	4262	984774	8255	0.4%	34.0%	0.9%
	1400	1121881	12517	4068	1117813	8449	0.4%	32.5%	0.7%
PI TM	1600	1218150	12517	4272	1213878	8245	0.4%	34.1%	0.7%
	1800	1285721	12517	4576	1281145	7941	0.4%	36.6%	0.7%
	2000	1335649	12517	4828	1330821	7689	0.4%	38.6%	0.7%
	200	126983	10269	5801	121182	4468	4.6%	56.5%	8.5%
	400	212631	10269	6635	205996	3634	3.1%	64.6%	6.0%
	600	283642	10269	7157	276485	3112	2.5%	69.7%	4.9%
	800	346990	10269	7527	339463	2742	2.2%	73.3%	4.2%
	1000	404689	10269	7725	396964	2544	1.9%	75.2%	3.7%
	1200	453426	10269	7908	445518	2361	1.7%	77.0%	3.4%
PI TM	1400	491786	10269	7968	483818	2301	1.6%	77.6%	3.2%
	1600	518079	10269	8153	509926	2116	1.6%	79.4%	3.1%
	1800	533761	10269	8111	525650	2158	1.5%	79.0%	3.0%
	2000	547686	10269	8052	539634	2217	1.5%	78.4%	2.9%